A Thesis
On

Development of a low loss Mn-Zn Ferrite Material for High Frequency Applications

Submitted in the partial fulfillment of requirement for the
Degree in

Master of Technology
IN

Materials Science and Engineering

Submitted by

KARUNA SAGAR CHATURVEDI
60702005

Under the guidance of

Prof. O.P. Pandey and Mr. Sameer Yadav

SCHOOL OF PHYSICS AND MATERIAL SCIENCE
THAPAR UNIVERSITY
PATIALA-147004, INDIA

June-2009

Dedicated to

My Loving Parents

CERTIFICATE

This is to certify that the thesis entitled, **"DEVELOPMENT OF A LOW LOSS MN-ZN FERRITE MATERIAL FOR HIGH FREQUENCY APPLICATIONS"**, submitted by **Mr. Karuna Sagar Chaturvedi** in the partial fulfillment of the requirement for the award of the degree of M. Tech in **Materials Science and Engineering** from the **School of Physics and Materials Science, Thapar University, Patiala**, is a record of candidate's own work carried out by him under our supervision and guidance. The matter embodied in this thesis has not been submitted in part or full to any other university or institute for the award of any degree.

The thesis work has been carried out from 01.01.2009 to 30.06.2009.

(Dr. O.P Pandey)
Prof. & Head
School Of Physics and Materials Science
Thapar University Patiala
Punjab (147004)

(Mr. Sameer Yadav)
Asst. Manager (R&D)
Cosmo Ferrites Limited
Jabli, Solan
Himachal Pradesh (173209)

Supervisors

Countersigned by:

Dr. O.P Pandey
Prof. & Head
School Of Physics and Materials Science
Thapar University, Patiala

Dr .R. K. Sharma
Dean, Academic Affairs
Thapar University, Patiala

ACKNOWLEDGEMENT

I visualize a rare movement of pride and pleasure to extend my sincere and heedful gratitude to my Guides **Dr. O.P Pandey, Professor and Head, School of Physics and Materials Science** and **Mr. Sameer Yadav, Assistant Manager, R&D, Cosmo Ferrites Limited** for their keen interest and valuable guidance, strong motivation and constant encouragement during the course of the work. I thank them from the bottom of my heart for providing me exposure to the latest research and developments in the field of Ferrite Materials. I, infact find paucity of words to express his sound knowledge of the subject and keen interest in it and his potential during the course of the work.

I am grateful to **Mr. Arun Yadav (G.M.), Cosmo Ferrites Limited**, for his encouragement, which will forever remain a driving force for me.

My greatest thanks are to **Dr. K.K.Raina**, **Deputy Director Thapar University** and **Dr. N. K. Verma, Dean Student Affairs Thapar University** for their full motivation and appreciation to my work. They provide me moral support as well as necessary help during my experimental work.

I am highly greatful to **Dr. Kulvir Singh**, **Asst. Prof. School Of Physics And Material Science, Thapar University Patiala (Punjab)** for his kind help and valuable suggestions and special attention throughout my work. It is due to his moral encouragement, love and providing me fountain of inspiration, all sorts of assistance from time to time into up-bringing me up to this stage.

I wish to express thanks to Mr. Ashish Gautam, Mrs. Lata Katoch, Mr. Arun Kumar, Mr. Charanjeet, Mr. Hemraj and all members of R&D, Cosmo Ferrites Limited, who give their support during my experimental work.

I wish to express my warm and sincere thanks to all my friends who devoted their valuable time and helped me in all possible ways towards successful completion of this work. Thanks are very small words for my dearest friends Mr. Sandeep Kumar Singh, Mr. Arun Kumar

Singh, Mr. Manjeet Sharma and Mr. Neetesh Kumar whose ideas and concepts have had a remarkable influence on my understanding in the field of Material Science and Engineering.

I would like to thank my parents, brother, sisters, and my whole family whose honest support and obstinate love give me energy to complete this work successfully and gave me untiring help during my difficult moments.

Date: 01-07-2009

Place: Patiala

Karuna Sagar Chaturvedi

(Roll.No.-60702005)

Abstract

Ceramic ferrites are magnetic materials composed of selected oxides with iron oxides. The most common commercial soft magnetic materials are Mn-Zn ferrites, having general formula AB_2O_4. The Manganese-Zinc ferrite is preferred for lower frequency applications generally for power transformers, power inductors and general power applications.

With the advance of modern electronic technology, there has been a critical need for Mn-Zn ferrites with lower power loss at higher frequencies. In keeping with the current demand for size reduction of electronic equipment, more power-saving electronic devices and more efficient switched-mode power supplies has received considerable attention. Power supplies being an integral part of electronic equipments from computers and microprocessors to TV and video tape-recorders, the demand for ferrites cores, which are an essential component of the switching power supplies, has increased.

In the present work, attempts have been made to reduce the power loss at high frequency, its variation with temperature in Mn-Zn ferrites, using traces of additives. The effect of these additives on the electrical and magnetic properties is studied intensively. In this project, Mn-Zn ferrite cores of the basic composition of 52.5 mole % Fe_2O_3, 41.2 mole % MnO and 6.3 mole % ZnO have been synthesized by conventional ceramic route. These ferrites have been investigated for their electrical and magnetic properties such as saturation magnetization, initial permeability, Curie temperature, resistivity and dielectric loss between 0.5MHz-3MHz. The minimum power loss of the Mn-Zn ferrite is 137 Kw/m3 at 100 KHz, 80^{o}C and 100 mT, and of 309 Kw/m^3 at 200 KHz, 100^{o}C and100 mT.

CONTENTS

LIST OF TABLES

List of Figures

CHAPTER 1

INTRODUCTION

1.1 History

In the recent times, iron and its alloys were used as magnetic materials for the applications in the electrical industry. However, with the discovery of higher frequencies, the customary techniques to reducing eddy current losses, using lamination or iron powder cores, were no longer efficient or cost effective.

This realization stimulated a renewed interest in "magnetic insulators" as first reported by S. Hilpert in Germany in 1909. It was readily understood that if the high electrical resistivity of oxides could be combined with desired magnetic characteristics, a magnetic material would result that was particularly well suited for high frequency operation.

These materials are called ferrites which have general formula MFe_3O_4 where M is the divalent ion like Zn^{++}, Mn^{++}. Research in order to develop this type of material, was undertaken in various laboratories all over the world, such as by V. Kato, T. Takei, and N. Kawai in the 1930's in Japan and by J. Snoek of the Philips Research Laboratories in the period 1935-45 in the Netherlands. By 1945 Snoek had laid down the basic fundamentals of the physics and technology of practical ferrite materials. In 1948, the Neel theory of ferromagnetic provided the theoretical understanding of this type of magnetic material.

These ferrites are homogeneous, ceramic materials composed of various oxides with iron oxide as their main constituent. Based upon the chemical composition, soft ferrites can be divided into two major categories, manganese-zinc ferrites and nickel-zinc ferrites. In each of these categories many different Mn-Zn and Ni-Zn material grades are being manufactured by varying the chemical composition or by different manufacturing techniques. The two families of Mn-Zn and Ni-Zn ferrite materials complement each other and allow the use of soft ferrites from audio frequencies to several hundred mega-hertz. The first practical application of soft ferrite was in inductors which was used in LC filters in frequency division multiplex equipment. The combination of high resistivity and good magnetic properties made these ferrites an excellent core material for these filters operating over the 50-450 kHz frequency range. The large scale introduction of TV in the 1950's was a major opportunity for the fledgling ferrite industry. In TV sets,

ferrite cores were the material of choice for the high voltage transformer and the picture tube deflection system. For four decades ferrite components have been used in an ever widening range of applications and in steadily increasing quantities, a few are mentioned in table-1 below.

Table 1.1 Applications of Soft ferrites.

Magnetic device	**Applications**
Power transformers and Chokes	High frequency power supplies
Inductors and tuned transformers	Frequency selective circuits
Pulse and wide band transformers	Matching devices
Magnetic deflection structures	TV sets and monitors
Recording heads	Memory storage devices
Rotating transformers	VCR's
Transducers	Vending machines and ultrasonic cleaners

Table 1.2 Merits and demerits of ferrites over other magnetic materials.

Advantages	**Disadvantages**
High resistivity	Low saturation flux density
Wide range of operating frequencies	Poor thermal conductivity
Low loss combined with high permeability	Low tensile strength
Time and temperature stability	Brittle material
Large material selection	
Versatility of core shapes	
Low cost	

These cubic ferrites are especially useful due to two key characteristics:

- High magnetic permeability, which concentrates and enhances the magnetic field.
- High electrical resistivity, which ensures total penetration of the electromagnetic (EM) field.

Furthermore, the dominance of ferrites rests upon a remarkable flexibility in providing tailor-made solutions, ease of fabrication, and price and performance considerations. Hence ferrites are widely manufactured into circuit elements like inductors and cores, reading-writing heads and information storage media.

Amongst the soft ferrites, Manganese Zinc Ferrites are most common, and are used in many more applications than their counterparts, such as nickel-zinc ferrites. Within the Mn-Zn category, large varieties of materials are possible and the material selection is mainly a function of the application that needs to be accommodated. The application dictates the desirable material characteristics which in turn determine the chemical composition of the ferrite material. Manganese zinc ferrites are primarily used for frequencies less than 2 MHz. Figure 1.1 shows the composition diagram for Mn-Zn ferrites in mole% for Ferric oxide, Manganese oxide and Zinc oxide. It identifies the composition which gives optimum performance for saturation flux density (B_s), low losses (Q) and high initial permeability (μ_i). It also identifies the Curie temperature (T_C) lines for 100 and 250°C. From this composition chart, it is clear that not one composition, of Mn ferrite, can fulfill all design objectives.

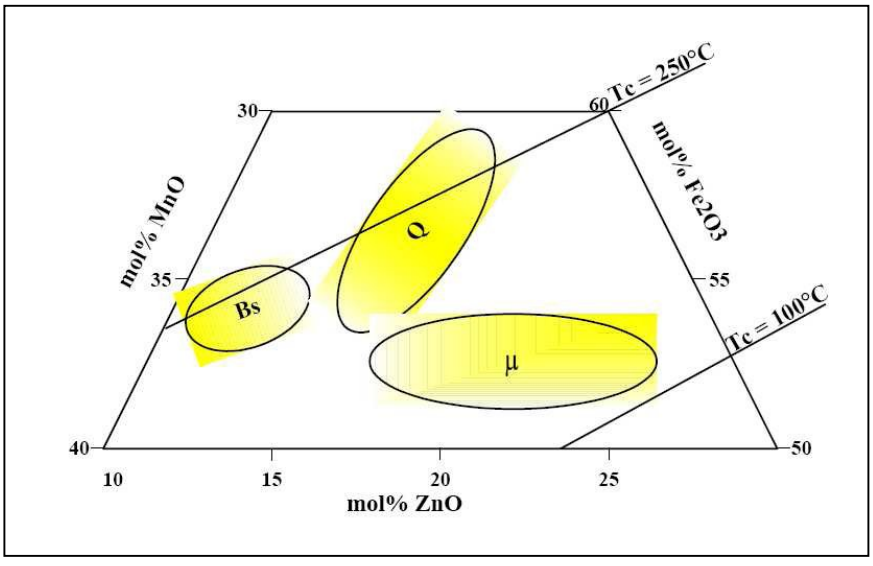

Figure 1.1 Composition Diagram for Mn-Zn ferrites [1].

B_s - Compositions of Higher Saturation

Q - Compositions of Higher Q

μ - Compositions of Higher Initial Permeability

Nickel Zinc ferrites are characterized by their high material resistivity which is several orders of magnitude higher than Mn-Zn ferrites. Because of its high resistivity Ni-Zn ferrite is the material of choice for operating from l-2 MHz to several hundred MHz. To cover such a wide frequency range and different applications, a large number of nickel-zinc materials have been developed over the years. Use of Nickel Zinc ferrites is limited due to their increasing cost. It should be noted that certain nickel chemistries are stress sensitive and can be adversely changed by some types of stress; this may be a mechanical shock or any grinding operations. Strong magnetic fields from holding devices and fixtures or magnetic chucks used in machining operations may also provide this stress. These resulting changes can include variation in permeability and core loss (lowering of Q). These changes cannot be reversed by degaussing or other electric/magnetic processes.

Manganese Zinc ferrite has the highest permeability and saturation induction of the ferrite class of materials and has the advantage of various stoichiometries with nearly zero magneto-crystalline anisotropy and magneto-restriction, important for stress insensitivity and low noise.

1.2 Crystal Structures of Ferrites

Ceramic magnets have become firmly established as electric and electronic engineering material; most contains iron as a major constituent and are collectively called ferrites. From the point of view of electric properties these are semi-conductors or insulators, in contrast to metallic magnetic materials which are electric conductors. Consequence of this is that the eddy currents produced by the alternating magnetic fields which many devices generate are limited in ferrites by their high intrinsic resistivities. Magnetic structures of increasing complexity starts from the spinning and orbital motion of electron, progressing to atom, and finally focus on domain. Although domain is important in explaining cooperative magnetic phenomena, the next larger physical magnetic entity after the ion is ferrite unit cell or crystal structure [1].

The crystal structure of ferrites can be regarded as an interlocking networking of positively charged metal ions (Fe^{3+},M^{2+}) and negatively charged divalent oxygen ions (O^{2-}).The arrangement of the ions or the crystal structure of the ferrite plays an important role in determining the magnetic interactions.

1.3 Classes of Crystal Structures in Ferrites

In ferrites, the crystal structure preferred is determined on the basis of size and charge of the metal ions that balance the charge of oxygen ions and the relative amounts of these ions. There are three crystal structures mostly available in case of ferrites. These are:

- Spinal Structure
- Garnet structure
- Hexa-ferrite structure

1.3.1 Spinal structure

The spinal is by far the most widely used ferrites. The spinal structure is derived from the mineral spinal ($MgAl_2O_4$ or $MgO.Al_2O_3$) whose structure was elucidated by Bragg. Analogous to the mineral spinal the magnetic spinal have general formula $MO.Fe_2O_3$, where M is divalent metal ion. The trivalent aluminum is usually replaced by Fe^{+++} or Fe^{+++} in combination with any other trivalent ion. Although the great majority of ferrites contain iron oxide as name implies, but there are some "ferrites" based on Cr, Mn, and other elements. Although Mn, Cr are not ferromagnetic elements, in combination with other elements such as oxygen and other metal ions, they can behave as magnetic ions.

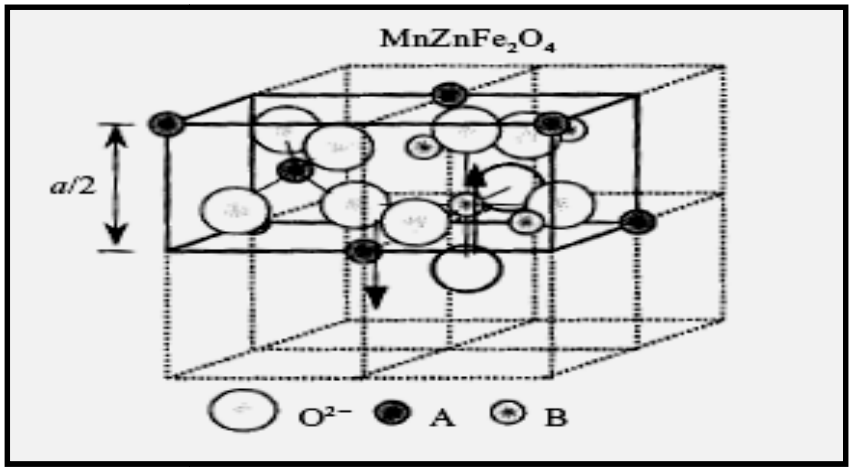

Figure 1.2 structure of Mn-Zn Ferrite.

Ion Charge Balance and Crystal structure

The spinal lattice is composed of a close packed oxygen arrangement in which 32 oxygen ions form a unit cell which is the smallest repeating unit in crystal network. Between the layers of oxygen ions, there are the interstices that may accommodate the metal ions. Not all the interstices are same; some which would be called **A** sites are surrounded with four nearest neighboring oxygen ions and are called tetrahedral sites. The other type of sites (B sites) is coordinated by six neighboring oxygen ions whose centre connecting lines describe an octahedron. The **B** sites are called octahedral sites. In the unit cell of 32 oxygen ions there are 64 tetrahedral sites and 32 octahedral sites. If all the sites are filled with metal ions, of either +2 or +3 valence, the positive charge would be much greater than the negative charge and so the structure will be much greater than negative charge. Due to which the structure will be electrically neutral. It turns out that of the 64 tetrahedral sites, only 8 are occupied and out of the 32 octahedral sites, only 8 are occupied. If , as in the mineral spinal the tetrahedral are occupied by divalent ions and the octahedral sites are occupied by the trivalent ions, the total positive charge will be $8\times(+2) = +16$ plus the $16 \times (+3) = +48$, or a total of +64 which is needed to balance the $32\times(-2) = -64$ for the oxygen ions. Then there would be eight formula units of $MO.Fe_2O_4$ [1].

The divalent ions are generally larger than the trivalent, octahedral sites are also larger than tetrahedral, therefore it would be reasonable that trivalent ions go into tetrahedral sites and divalent goes to the octahedral sites.

Site Preference of the Ions

The preference of the individual ions for two types of lattice sites is determined by:

The ionic radii of the specific ions

The size of interstices

Temperature

The orbital preference for specific coordination

Table 1.3 Metal ions involved in Spinal ferrites [1]

Metal Ions	Ionic Radius (Angstronm Units, A^0)
Mg^{++}	0.78
Mn^{++}	0.91
Mn^{+++}	0.70
Fe^{++}	0.83
Fe^{+++}	0.67
Co^{++}	0.82
Ni^{++}	0.78
Cu^{++}	0.70
Zn^{++}	0.82
Cd^{++}	1.03
Al^{+++}	0.57
Cr^{+++}	0.64

Two exceptions are found in Zn^{++} and Cd^{++} which prefer tetrahedral sites because electronic configuration is favorable for tetrahedral bonding to oxygen ions.

(a) Normal Spinals

In a unit cell of spinal lattice, eight tetrahedral and sixteen octahedral sites are occupied by metal ions. In case of mineral spinals the divalent ion (Mg) occupy the **A** site and trivalent ion (Al) occupy the **B** sites, this is known as normal spinal.

(b) Inverse Spinals

In many cases in which the trivalent ions preferred the **A** sites and filled these first. Spinals showing this type of structure are known as inverse spinals.

1.3.2 Hexagonal Ferrites

This class of magnetic oxide is called megnetoplumbite structure from the mineral of the same name. Whereas the symmetry of the spinal crystal structure is cubic, that for the megnetoplumbite structure is hexagonal. Thus, it has a major preferred axis called **C** axis. The preferred direction is used to good advantage for permanent magnetic material.

The megnetoplumbite unit cell contains a total of ten layers, two of which contain M^{++} ion: four layers of oxygen ions each: followed by a layer of three oxygen ions and one M^{++} ion; again followed by four oxygen layers of four ions each: and another layer containing the three oxygen ions and one M^{++} ion but situated diametrically opposite to the M^{++} ion in the previous layer containing M^{++}.

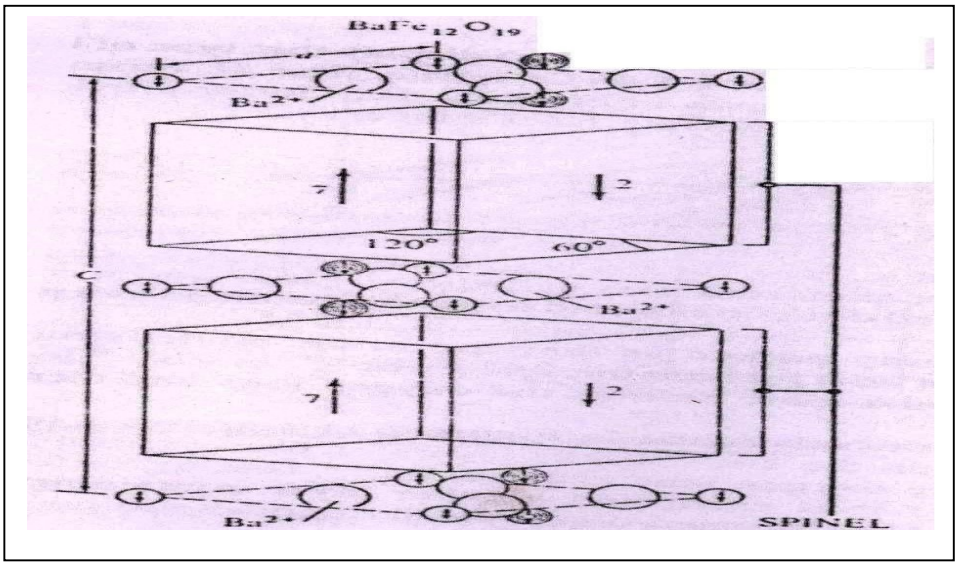

Figure 1.3 Crystal Structure of Hexagonal Mn-Zn Ferrite.

The Fe^{+++} ions are located in the interstices of these ten layers. There are octahedral and tetrahedral sites, as well as one more type not found in the spinal structure in which the metal ion is surrounded by five oxygen ions forming a trigonal bi pyramidal in the same layer of the M^{++} ion.

The megnetoplumbite formula is $MFe_{12}O_{19}$, where M can be Ba, Sr, or Pb. There are two formula units per unit cell. Per formula unit, the moments of the 12 Fe^{+++} ions are arranged with the spins of 12 in the up direction and 8 in the down direction, giving a predicted net moment of 4 Fe^{+++} ions per formula unit time 5 per ion, or a total of 20 per formula unit.

1.3.3 Magnetic rare earth garnets

Magnetic garnets crystallize in the dodecahedral or 12-sided structure related to the mineral garnet. The general formula is $3M_2O_35Fe_2O_3$ or $M_3Fe_5O_{12}$. In this case all the metal ions are trivalent in contrast to the other two classes. In the important magnetic garnet, M is usually yttrium (Y) or one of the rare earth ions. Even though yttrium is not a rare earth ion, it behaves as one and therefore is included in the designation rare earth garnets. The ions La^{+++}, Ca^{+++}, Pr^{+++}, and Nd^{+++} are too large to form simple garnets but may form solid solutions with other rare earth garnets.

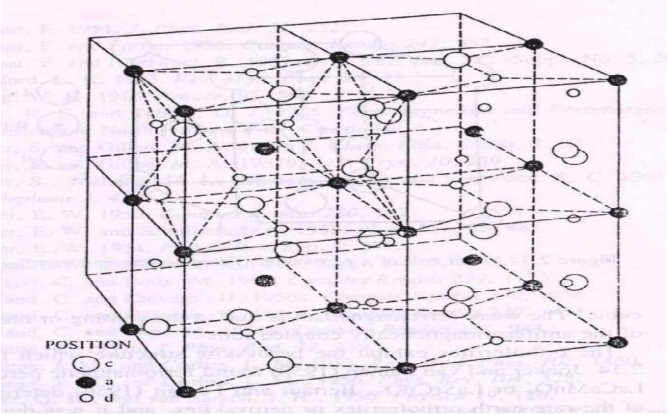

Figure 1.4 Crystal Structure of Magnetic rare earth garnet.

Magnetic garnets were discovered by Bertaut and Forrat and independent by Geller and Gaileo at about the same time. The crystal structure of magnetic garnets was elucidated by Geller and Gilleo. There are three different types of sites for garnets (a) tetrahedral (b) octahedral; and (c) dodecahedral sites. The unsubstituted garnets that have only trivalent ions are very stoichiometric, so that they involve fewer preparation problems compared to the spinels.

The rare earth ions are large, and so they occupy the large dodecahedral sites. There are 16 octahedral, 24 tetrahedral, and 24 dodecahedral sites in a unit cell containing eight formula units. One formula unit, $3M_2O_35Fe_2O_3$, is distributed as follows:

$3M_2O_3$ –dodecahedral (c)

$3Fe_2O_3$ –tetrahedral (a)

$2Fe_2O_3$-octahedral (d)

The moments of the Fe^{+++} ions on the octahedral sites are antiferromagnetically coupled to the moments of the Fe^{+++} ions on the tetrahedral sites. Similarly, moments of the M^{+++} ions on the dodecahedral sites are also coupled to the tetrahedral sites and, as previously

mentioned, may contribute to the magnetization of that sublattice. In the absence of the rare earth ion contribution as in the most important of the series, $3Y_2O_3.Fe_2O_3$, all the moments are due to the Fe^{+++} ions.

1.4 The nature of domains

A magnetic domain describes a region within a material which has uniform magnetization. This means that the individual moments of the atoms are aligned with one another. The regions separating magnetic domains are called domain walls where the magnetization rotates coherently from the direction in one domain to that in the next domain. The size and shape of a domain may be determined by the minimization of several types of energies. They are;

a). Magnetostatic energy

b). Magnetocrystalline anisotropy energy

c). Magnetostrictive energy

d). Domain wall energy

a). Magnetostatic Energy

The magnetostatic energy is the work needed to put magnetic poles in special geometric configurations. It is also the energy of demagnetization. It can be calculated for simple geometric shapes. For an infinite sheet magnetized at right angles to the surface the equation for the magnetostatic energy per cm^3 is;

$$F_p = 2\pi M_s^2$$

Neel and Kittel have calculated the magnetostatic energy of flat strips of thickness, d, magnetized to intensity, M, alternately across the thickness of the planes. The equation is;

$$E_p = 0.85\ dM^2$$

The calculations for other shapes come out with the general formula;

$$E_p = (\text{Constant})\ x\ dM_s^2$$

Therefore the magnetostatic energy is decreased as the width of the domain de-creases.This mathematically confirms the assumption that the splitting of domains into smaller widths decreases the energy from the magnetostatic view. In fact, the energy of the domain structure is one thousandth that of a similar sized single do-main.

b). Magnetocrystalline Anisotropy Energy

Most matter is crystalline in nature; that is, it is composed of repeating units of definite symmetry. When a common geometrical configuration is considered it may form the smallest repeating unit, namely a cube. Atoms or molecules are usually located at corners of the cube and in addition, at either the center of the cube or at the centers of the 6 faces. In most magnetic materials, to varying degree, the domain magnetization tends to align itself along one of the main crystal directions. This direction is called the easy direction of magnetization. Sometimes it is an edge of the cube and at other times, it may be a body diagonal. The difference in energy of a state where the magnetization is aligned along an easy direction and one where it is aligned along a hard direction is called the magnetocrystalline anisotropy energy. This magnetocrystalline anisotropy energy is also that needed to rotate the moment from the easy direction to another direction. The energy of the domain can be lowered by this amount by having the spins (ferromagnetics) or moments (ferrimagnetics) align themselves along these directions of easy magnetization. In materials with high uniaxial anisotropy energy the moment of one domain is usually aligned along an easy direction of magnetization. Then, the adjacent domain will have the same tendency to align along the same axis but in the opposite direction. Even in materials with lower anisotropy, the 180° wall is often found. In crystals of cubic symmetry, where many of the major axes are at right angles(such as the cube edges) the 90° domain wall is also a reasonable possibility.

Magnetocrystalline anisotropy is due to the fact that there is not complete quenching of the orbital angular momentum as we postulated originally. With a small orbital moment that is mechanically tied to the lattice, the spin system can couple to it and therefore indirectly affect the lattice or the dimensions of the material.

c). Magnetostrictive Energy

When a magnetic material is magnetized, a small change in the dimensions occurs. The relative change is on the order of several parts per million and is called magnetostriction.

The converse is also true. That is, when a magnetic material is stressed, the direction of magnetization will be aligned parallel to the direction of stress in some materials and at right angles to it in others. The energy of magnetostriction depends on the amount of

stress and on a constant characteristic of the material called the magnetostriction constant.

$$E = 3/2\ \lambda\sigma$$

Where; λ = magnetostriction constant

σ = Applied stress

The convention of the sign of the magnetostriction constant is such that if the magnetostriction is positive, the magnetization is increased by tension and also the material expands when the magnetization is increased. On the other hand, if the magnetostriction is negative, the magnetization is decreased by tension and the material contracts when it is magnetized. Magnetostriction as in the case of anisotropy is due to incomplete orbital quenching and the so-called spin-orbit, L-S or Russell Saunders coupling [1]. Stresses can be introduced in ferrites by mechanical and thermal operations such as firing, grinding, and tumbling. These stresses also affect the directions of the moments locally depending on the distribution of the stresses.

d). Domain Wall Energy

Although Weiss first came up with the idea of the strong molecular field producing regions of oriented atomic moments or of spontaneous magnetization, it was Blochwho was the first to present the idea of magnetic domains, with domain walls (sometimes called Bloch walls) or boundaries separating them. In the domain structure of bulk materials, the domain wall or boundary is that region where the magnetization direction in one domain is gradually changed to the direction of the neighboring domain. If 5 mm is the thickness of the domain wall which is proportional to the number of atomic layers through which the magnetization is to change from the initial direction to the final direction, the exchange energy stored in the transition layer due to the spin interaction is;

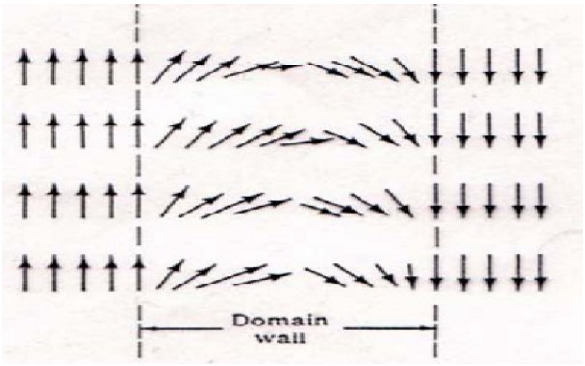

$$E_e = kT_c/a$$

where kT_c = Thermal energy at the Curie point

a = Distance between atoms

Therefore the exchange energy is reduced by an increase in the width of the wall or with the number of atomic layers in that wall. However, in the presence of an anisotropy energy or preferred direction, rotation of the magnetization from an easy direction increases the energy so the wall energy due to the anisotropy is:

$$E_k = k\,\delta$$

In this case, the energy is increased as the domain width or number of atomic layers is increased. The two effects oppose each other and the minimum energy of the wall per unit area of wall occurs according to the following equation;

$$E_w = 2(K_a T_c/a)^{1/2}$$

where K_a = Anisotropy constant (described later)

If magnetostriction is a consideration, the equation is modified to;

$$E_w = 2(kT/a)^{1/2}\,(K_a + 3\lambda_s \sigma/2)^{1/2}$$

Where λ_s = magnetostriction constant

Typical values of domain wall energies are on the order of 1-2 ergs/cm^2 the domain wall thickness for the condition of minimum energy is given by the equation;

$$\delta = (\text{Constant}) \times a(E/K)^{1/2}$$

Typical calculated values of δ are about 10^3 Å or about 10^{-5} cm. With some soft magnetic materials the value may be about 10^{-6} cm while in some hard materials, the value may be on the order of $l0^{-4}$ cm. or about one micron. The whole array of domains will be arranged in such a way as to minimize the total energy of the system composed mainly of the above four energies.

1.5 Hysteresis behavior

In magnetic applications, the interest is to know the amount of induction which applied field creates. In soft magnetic materials, a high induction for a low field is required. In this case, H is very small compared to 4 π M and B is essentially equal to 4πM. In the case of a permanent magnet, the H component can amount to from 50% or more of the total B. The increase the magnetic field, the induction increases as shown in Figure 1.5 for demagnetized specimen. At high fields, the induction flattens out at a value called the saturation induction, Bg. If, after the material is saturated, the field is reduced to zero and then reversed in the opposite direction, the original magnetization curve is not reproduced but a loop commonly called a hysteresis loop is obtained. Figure 1.5 shows such a hysteresis loop with the initial magnetization curve and hysteresis loop magnetization curve included. The arrows show the direction of travel. We notice that there is a lag in the induction with respect to the field. This lag is called hysteresis. As a result, the induction at a given field strength has 2 values and cannot be specified without a knowledge of the previous magnetic history of the sample. The area included in the hysteresis loop is a measure of the magnetic losses incurred in the cyclic magnetization process [2].

The hysteresis losses can also be correlated with the irreversible domain dynamics as mentioned previously. The value of the induction after saturation when the field is reduced to zero is called the remanent induction or remanence or retentivity, (B_r). The values of the reverse field needed after saturation to reduce the induction to zero is called the coercive force or coercivity, (H_c)

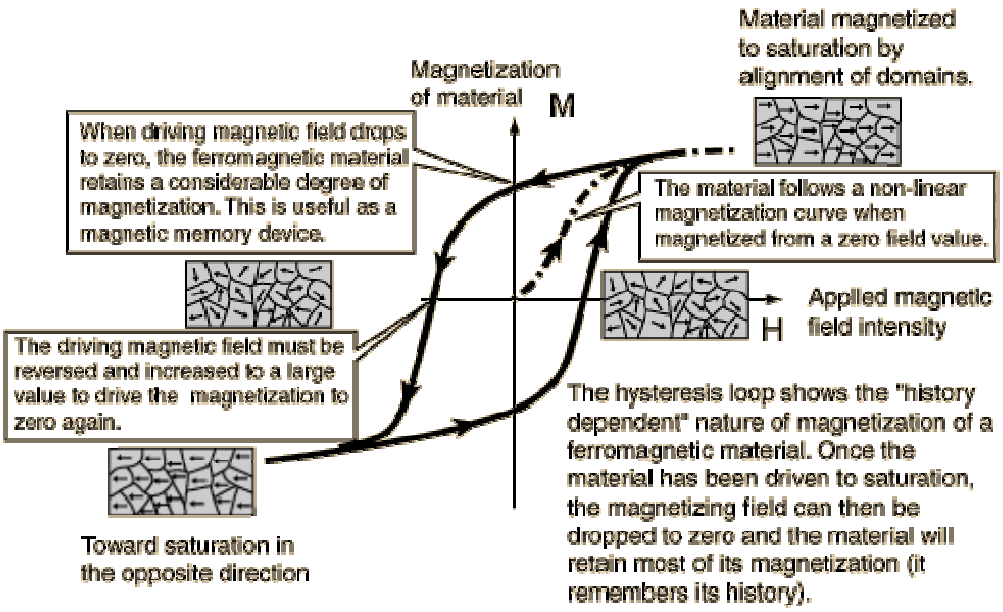

Figure 1.5 Initial magnetization curve and hysteresis loop [2].

The unit for H_C is the oersted and that for B_r is the gauss. Both of these properties are very important and will be referred in almost every magnetic application.

CHAPTER 2

LITERATURE REVIEW

The development and continued success of switch-mode power supplies is constantly challenging the ferrite industry to produce new, high-quality ferrite cores capable of operating at increasingly higher frequencies [1]. For this reason it is important to reduce the power losses of Mn-Zn ferrites that are used as transformer cores.

The electromagnetic characteristics of Mn-Zn ferrite are not only dependent on the composition of the main elements but also on the material's microstructure [2]. As a consequence of this, efforts have been made to improve their loss characteristics by controlling the size of the grains and the distribution of the small amounts of additives in the grain-boundary region [3]. In Mn-Zn ferrites the grain boundaries exhibit different chemical and physical properties than the ferrite grains. The segregation of impurities and the partial re-oxidation of the Fe^{2+} on the grain boundaries during cooling make the Mn-Zn-ferrite grain boundaries highly insulating in comparison to the grain interior. These insulating layers are, in practice, very thin and therefore exhibit a relatively high electrical capacity.

Core loss can be divided into three components: hysteresis loss (P_h), eddy-current loss (P_e) and residual loss (P_r). The proportions of these components in the total loss can vary widely, depending on the measurement conditions such as frequency and magnetic flux density. At low frequencies P_h losses are dominant, and in order to reduce these losses it is important to form a uniform microstructure that is free from lattice defects and pores. At high frequencies the proportion of P_e losses increases, but this can be reduced by increasing the resistance of the cores. Eddy-current loss can be decreased by having grain boundaries with a high electrical resistance and by having a ceramic microstructure with small grains. The resistance of the grain boundaries is determined by additives, which are enriched at the grain boundaries during the sintering process, forming an insulating phase. Small grains can be achieved by applying sintering conditions that suppress the grain growth and by choosing additives that act as grain- growth inhibitors.

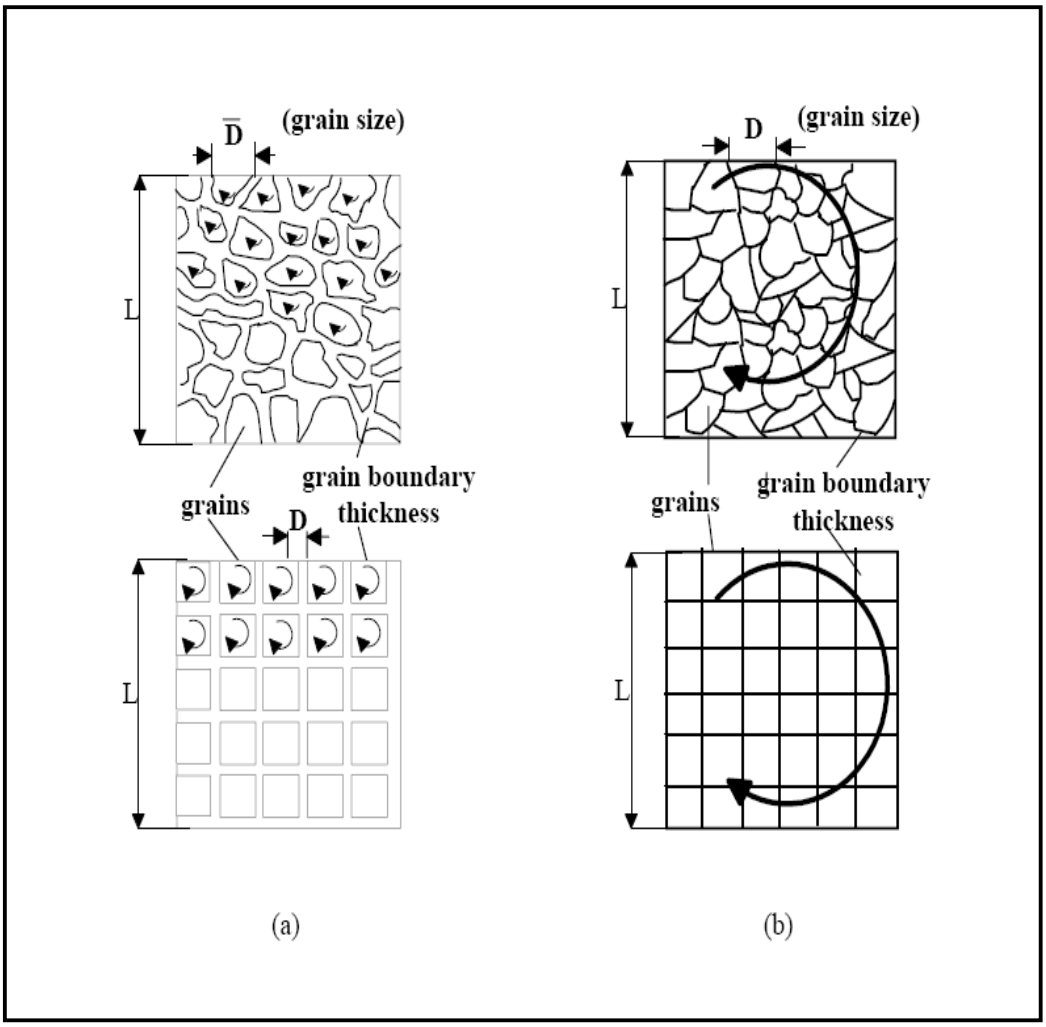

Figure 2.1 Brick-wall-microstructure models: (a) schematic picture of a real and an ideal Microstructure of a material with isolated magnetic grains exposed to micro-eddy currents. (b) A sketch of an actual and an idealized ferrite microstructure with grain boundaries permeable to the eddy current. [4]

In general, two extreme cases regarding the eddy current in the magnetic core of Mn-Zn ferrites can be identified by applying the brick-wall model [4].

In the first case, when the magnetic grains are isolated and the eddy current in this hypothetical case is localized inside the grains, Figure 2.1 (a), the core behaves as an assembly of individual magnetic grains in which each grain contributes to the eddy-current loss.

A different dependence between the total loss and the microstructure hold when the grain boundaries are permeable to the eddy current, Fig. 2.1 (b). According to this model the bulk material can be approximated by a group of small cubes of size D, separated by high-resistance layers of thickness δ_{gb} and resistance R_{gb}.

Using this model, at low frequencies ($\omega cR << 1$),

$$P_e = cB_m^2 f^2 \cdot \frac{D}{R_{g.b.}^{(mic)}}$$

And at high frequencies ($\omega cR >> 1$), the equivalent relation is

$$P_E \approx \propto \varepsilon_{g.b.} \frac{D}{\delta_{g.b.}}$$

Thus, the eddy-current power loss Pe, which prevails in the frequency range above 500 kHz, can be effectively suppressed by decreasing the average grain size (D), by increasing the grain-boundary resistance and by increasing the grain-boundary width δ_{gb}.

In the switching power supplies used in various types of electronic equipment, technological innovation is moving toward smaller size and higher performance. The core losses of Mn-Zn ferrite are composed of hysteresis losses, eddy current losses and residual losses. When the switching frequency range widens to 100 KHz through 1 MHz, these three kinds of losses relative to each frequency differ. The effect of composition and trace additives on the above core loss factor in each frequency range and effects of manufacturing conditions (mainly on grain structure control) were quantitatively analyzed, and lower losses were obtained by optimizing the fallowing five factors [5]:

(1) Average grain size and grain size distribution in the core
(2) Sintered density and pore distribution in the core
(3) Formation of a high –resistivity phase at grain boundaries by trace additives
(4) Homogeneity of composition and components
(5) Residual stress

Ke Sun *et al.* [6] have studied the Manganese–zinc (Mn-Zn) ferrites doped with NiO addition which were prepared by solid-state reaction method. Losses (P_L) were divided into hysteresis loss (P_h), eddy current loss (P_e) and residual loss (P_r), temperature and frequency characteristics of each loss, and the ratio of each loss to the total losses have been discussed. P_h increased monotonously with increasing NiO, and its variation can be

explained by the relation: $P_h \alpha 1/\mu^3_i$. P_e first reduced before achieving its minimum, and then rose gradually. The variation of P_e was not consistent with the classical expression, $P_{e,cl} \alpha D^2/\rho$, with D as grain size, and the excess loss (Pe, exc) can contribute to the Pe. Finally, the sample doped with 0.10 wt. % NiO showed the lowest losses of 175 kW/m^3 at 100 °C, 0.5MHz and 50 mT, and of 207 kW/m^3 at 100 °C, 1MHz and 30 mT [6].

Manganese–zinc (Mn-Zn) power ferrites are widely used as transformer core operated in the state of high power, which must be with high saturation induction (Bs), initial permeability (μ_i) and low losses (P_L). Besides the basic composition and sintering process [1–3], addition performs vitally here for it influences the losses of Mn-Zn ferrites significantly.

Recently, various additions, like CaO, SiO_2, TiO_2, SnO_2 and Nb_2O_5, have been reported to obtain more uniform microstructure, higher electrical resistivity (ρ), and lower losses (PL) [4–9]. The influences of NiO in the formula system on the structural and magnetic properties of Mn-Zn ferrite have been investigated in Ref. [10] while the basic formula system has four compositions of Fe_2O_3–MnO–ZnO–NiO. Singh et al. [7] have obtained high electrical resistivity (ρ), saturation magnetization (Ms) and low relative loss factor (tan δ/μi) Ni-substituted Mn-Zn ferrites processed by soft chemical technique.

Amarendra K. Singh et al. [7] have studied the high performance Ni-substituted Mn-Zn ferrites processed by soft chemical technique. DC resistivity, dielectric relaxation intensity, relative loss factor, Curie temperature, saturation magnetization and the *B-H* loop parameters have been studied. Resistivity and dielectric relaxation intensity are observed to increase and decrease, respectively, with increase in nickel content. The relative loss factor is observed to be in the range nearly of 10^2-10^4. Curie temperature is observed to increase continuously from 370° C to 490° C with increase in nickel content. Almost rectangular *B-H* curves and reasonably low coercivity are observed.

Y. Liu and Shijin [8] have reported that the advance of modern electronic technology, there has been a critical need for Mn–Zn ferrites with even higher permeability and even lower power loss at higher frequencies. In this study, ferrite with extremely low losses than conventional ferrite materials at high frequency was developed employing a conventional ceramic powder processing technique. As a result, the core loss at 3MHz, 10mT and at 100 °C is around 300kW/m^3, and its cutoff frequency is 4MHz.

The power loss (P_C) can be expressed as a function of frequency (f) and magnetic flux density (B):

$$P_C = kB^x f^y$$

Where x and y are called Steinmetz coefficients. Theoretically, the power loss in ferrites is generally split up into three contributions with quite different physical origins

$$P_C = P_h + P_e + P_r = K_H B^3 f + K_E B^2 f^2/\rho + P_r$$

Where P_C is the total power loss, P_h, P_e and P_r are the hysteresis loss, eddy current loss and residual loss, respectively, K_H and K_E are constants, B is the magnetic flux density, f is the frequency and r is the electrical resistivity.

Table 2.1 Important magnetic properties for new DMR50 material

Property	Measurement	Value
Initial permeability (μ_i)	25 ^{0}C; 10 kHz; <0.1 mT	1400
Amplitude permeability (μ_a)	25 ^{0}C; 25 kHz; 200 mT 100 ^{0}C; 25 kHz; 200 mT	2100 2300
Saturation magnetization (B_s, mT)	25 ^{0}C; 1194 A/m 100 ^{0}C; 1194 A/m	490 400
Power losses P_{cv} (mW/cm^3)	100 ^{0}C; 500 kHz; 50 mT 100 ^{0}C; 700 kHz; 30 mT 100 ^{0}C; 1 MHz; 30 mT 100 ^{0}C; 3 MHz; 10 mT	60 70 160 310
Curie temperature (^{0}c)		250

New DMR50 material exhibit very good power loss property during wide frequency range. Figure 2.2 shows the power losses of this new material as a function of temperature measured at different frequencies and different flux densities.

One can see from Fig. 2.2 that, at the measured temperature range [8], power losses of this material are less than 200 kW/m^3 in the frequency range 100 kHz–1 MHz, and are only around 300kW/m^3 under 3 MHz, 10mT and 100^{0}C, which is the highest. This new

material had extremely low core loss around 60kW/m^3 under the measurement condition of 500 kHz, 50mT and 100^{0}C. A summary of the important magnetic properties for this material are given in Table 2.1.

The resistivity of the grain boundaries of this material has been increased with the help of additives. To make this material suitable for frequencies around 1 MHz, the electrical resistivity of the material inside the grains has also been increased by adding appropriate dopants.

Through increasing the resistivity of the grains and also of the grain boundaries using TiO_2, Nb_2O_5 and ZrO_2, Pe is lowered. As P_h is also lowered by uniform microstructure and less voids, P_r is lowered by using fine grains as described above and will be seen later, total Pcv of this material is lowered.

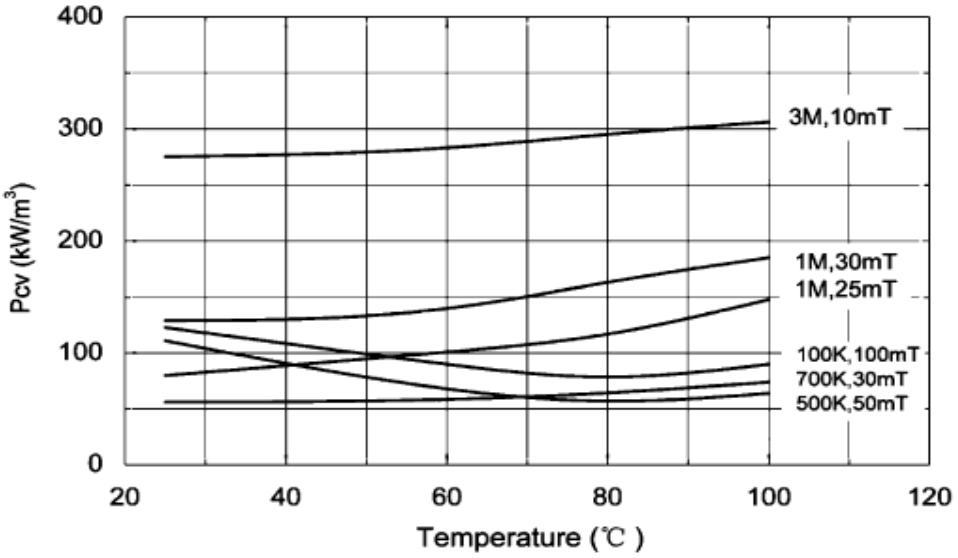

Figure 2.2 Power losses for various measuring conditions as a function of temperature [8].

Fig. 2.3 shows the power losses plotted as a function of frequency at various magnetic flux densities. A similar power loss behavior versus frequency is observed, regardless of magnetic flux density B. The power loss of this material increases with increasing frequency. It can be clearly seen that, when B is small, the power loss increases linearly in the low frequency range and then deviates from the linearly at above about 100 kHz, and then again deviates at above 500 kHz. These deviations from the linearity indicate that the constitution of total loss Pcv is different at different frequency ranges.

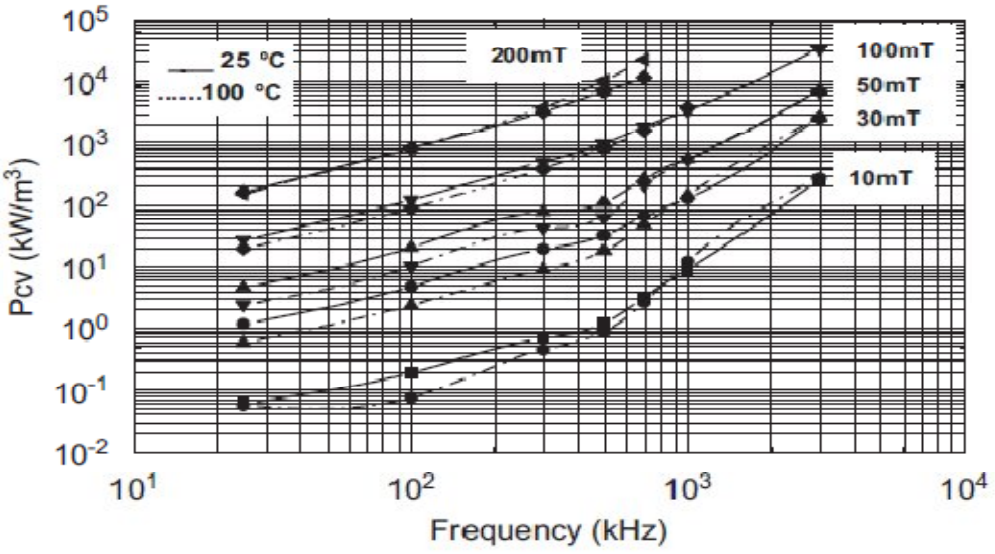

Figure 2.3 Power losses for various magnetic flux densities as a function of frequency at 25 and 100^0c.

The magnetic property of a magnetic material is closely related to its microstructure.

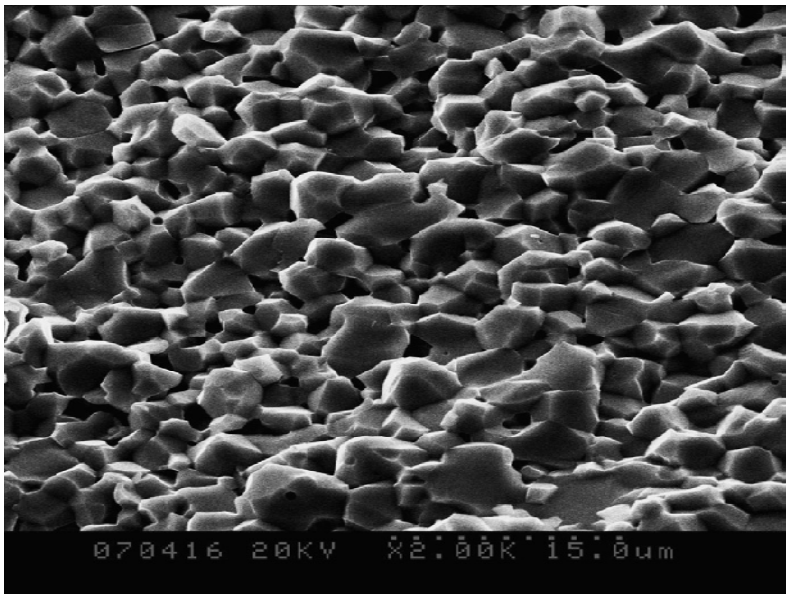

Figure 2.4 Typical SEM image of the microstructure of DMR-50 material [8].

The microstructure of this ferrite materials using SEM, is shown in Fig. 2.4. As we can see, the average diameter of the grain is about 2.55mm, which reduces the P_r in high

frequencies, and also makes the high peak of complex permeability. So if the grain size is small enough, Mn–Zn ferrites can also work at frequencies higher than 3 MHz we can also see from Fig. 2.2 that there also exist some voids, some larger and smaller grains, which indicate that there exist exaggerated grain growth.

R. Lebourgeois et al [9]. Reported that on High Frequency Mn-Zn Power Ferrites the influence on core losses of silica-calcia additions and Ti-substitutions for optimizing a power ferrite from *25* kHz up to 2 MHz Losses in magnetic materials have two main contributions: one is due to hysteresis and originates from the non-reversibility of the magnetization process, the other is dynamic and should be studied at a more macroscopic scale. For time harmonic fields, losses in magnetic materials can be depicted by a difference in phase between the external applied magnetic field and the resulting magnetization. Whatever it's physical origin, this time lag is closely related to magnetization mechanisms which occur in the material.
For soft ferrites, the main contributions to core losses are:

Hysteresis loss mainly due to the non-reversing domains walls displacements. This contribution exists in all magnetic materials. For dynamic applications, hysteresis loss could be estimated as the area of the quasi-static hysteresis loop times frequency. Hysteresis loss can be reduced by decreasing the coecitive field. This can be achieved by increasing the saturation magnetization MS, decreasing the internal stress, the magnetostriction and the magnetocrystalline anisotropy. For a polycrystalline ferrite, the porosity and mostly the intra-granular porosity must be kept as low as possible.

Eddy current loss due to electronic movements to cancel the applied magnetic field. This kind of loss is a part of the dynamic contribution. It is magnified in metallic magnetic materials where the electrical conductivity is high and is often negligible for most ferrites. For all magnetic materials, eddy current loss can be reduced by increasing the dynamic resistivity. Moreover, eddy current loss depends on the structure of the Weiss domains, so for polycrystalline ferrites such as Mn-Zn power ferrites, eddy current loss is microstructure dependent **[3].**

Resonance-relaxation loss due to either the reversible high frequency displacement of the domain walls or to the magnetization rotation inside a domain. It is another important part of the dynamic contribution which could dominate all other contributions if user

does not take care. A practical way for choosing a ferrite is to consider the complex permeability spectrum for determining the frequency range in which losses occur.

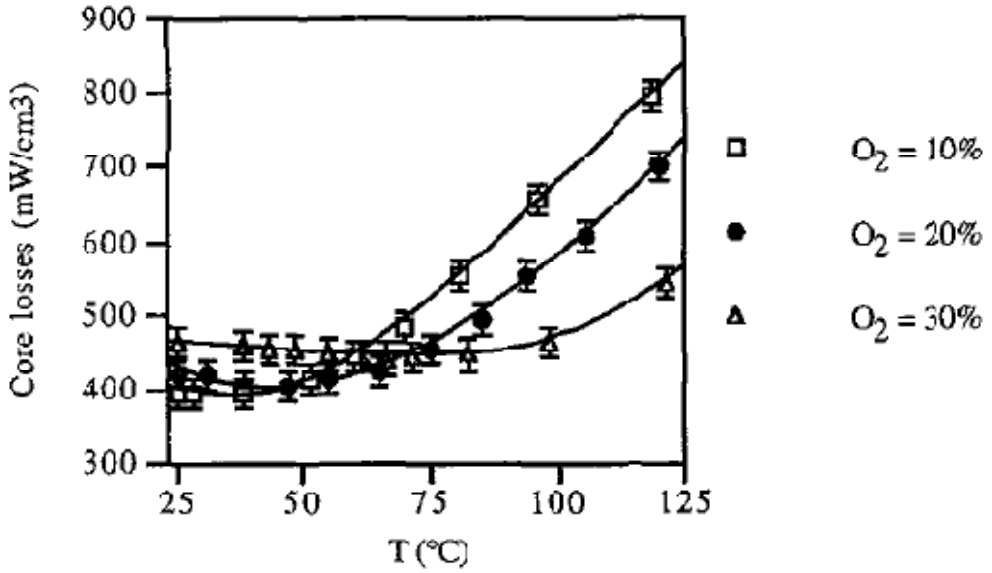

Figure 2.5 Core losses at 1 MHz and 50 mT versus temperature of a high frequency Mn-Zn power ferrite fired at 1200°C under various oxidation conditions (0_2 = 10, 20 and 30%)

YU Zhong et al. [10] have studied the effect of additives, such as CaO and V_2O_5 on the magnetic properties of high frequency Mn-Zn power ferrite is studied by the conventional ceramic process. As a result, the grain boundary resistivity increases and the power loss declines with the addition of CaO enriched at the grain boundary. By adding an optimum amount of V_2O_5 which acts indirectly via liquid phase formation and influences the microstructural development during sintering, the crystalline grain of ferrite was refined, the porosity decreases, the amount of grain boundary and the grain boundary resistivity increased, so the power loss is suppressed.

In keeping with the advance of more compact and more power-saving electronic equipment, the demand is increasing for smaller and more efficient switching power supply. Therefore, it is necessary to provide the adequate magnetic power ferrite materials to satisfy the demand. Such ferrite materials have to meet the following main requirement: 1) high initial permeability (μ_i); 2) high saturation magnetic induction (*Bs)*; 3) high Curie temperature (*Tc*); 4) high electrical resistivity (ρ); 5) low core power loss (P_L).

Znidarsic et al. [11] reported the effect of Ta_2O_5 in lowering the power loss at high frequencies in Mn-Zn ferrites. Ta_2O_5 was reported to inhibit the grain growth and increased electrical resistivity by segregating at the grain boundaries.

K. Ishino et al. [12] reported that hysteresis loss as well as eddy current loss decreased by the addition of Ta_2O_5. They regarded the reason for this fact as due to the relatively higher density of the ferrite at the same grain size by the addition of Ta_2O_5.

In 2003, S R Murthyi [13] have investigated the microwave sintering (MS) method which has been successfully used for densifying Mn–Zn ferrites used for high frequency applications. This method needs only a short time to obtain high density when compared to conventionally sintered (CS) Mn–Zn ferrites. The lowest power loss was also achieved at 100 kHz and 200 mT condition for the microwave sintered samples. Conductor-embedded ferrite transformers were constructed. Using CS and MS samples and output power, efficiency, and surface rise of temperature were measured at sinusoidal voltage of 25 V with frequency, 1 MHz the efficiency and surface rise of temperature of transformer were found to be high and low, respectively.

Weon Hee Jeong and Young Ho HAN [14] have studies on effects of Ni-substitution in Mn–Zn ferrites on power losses and electromagnetic properties. When NiO was substituted for MnO in the range from 0 to 8 mol%, lattice constants decreased gradually due to the smaller ionic radius of Ni ions. NiO substitution lowered the initial permeability and increased the Curie temperature. NiO substitution also suppressed the magnitude of the imaginary part of complex permeability in the high-frequency range (>1 MHz). The minimum power loss at 1MHz and 25mT moved to higher temperatures with NiO substitution. The sample with 4 mol% NiO showed the lowest power loss of 57 kW/m^3 at 80^0C, 1MHz and 25 mT.

Mn–Zn ferrites are widely used as transformer core materials for high-frequency switched mode power supplies. Materials with high electrical resistivity, high permeability and low power losses at high frequencies are required. The major concern for MHz-range applications is the power loss off ferrite cores, which comprises hysteresis loss, eddy current loss and residual loss. The residual loss of Mn–Zn ferrites has generally been ignored below the MHz range. Several studies recently revealed that the residual loss becomes more dominant in the MHz range.

Figure 2.6 shows the temperature dependence of initial permeabilities at various NiO contents. The initial permeability decreases with increasing NiO content at most of the temperatures studied, while addition of NiO increases Curie temperature. The permeability of polycrystalline ferrites can be described by the superposition of two different magnetizing processes:

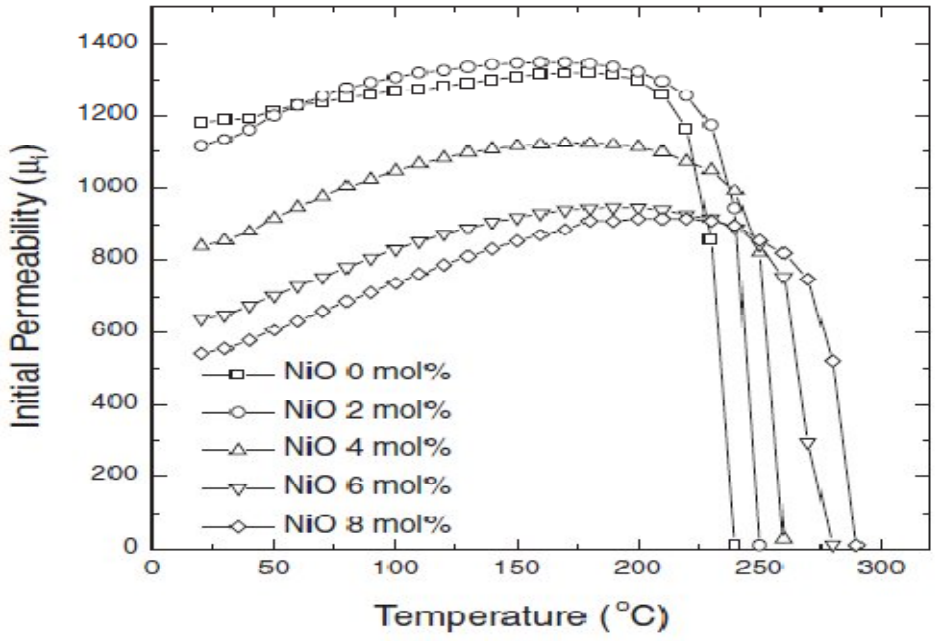

Figure 2.6 Temperature dependence of initial permeabilities at various NiO contents.

Spin rotation and domain wall motion. When grain size is smaller than 4 mm, the domain wall motion would be eliminated due to the absence of the domain wall. In general, the initial permeability for a polycrystalline Mn– Zn ferrite with saturation magnetization Ms and magnetocrystalline anisotropy constant k_1 is given as:

$$\mu_i = \frac{M_s^2}{ak_1 + b\lambda\sigma}$$

Where a and b are constants, λ is the magnetostriction constant and σ is the inner stress.

Figure 2.7 shows the temperature dependence of power losses at 25mT and 1MHz. The temperature dependence of power losses is improved with increasing NiO content. The specimens with 2 mol% NiO or less exhibit a monotonic increase in power losses as

temperature increases above room temperature. As NiO content becomes greater than 4 mol%, we observe negative temperature dependence at lower temperatures and a positive behavior at higher temperatures, separated by a power loss minimum. The sample with 4 mol% NiO shows the minimum power loss of 57 kW/m^3 at 80^{0}C, 25mT and 1 MHz. The temperature (Tmin) at which the minimum power loss occurs should preferably be about 80^{0}C, because the transformer core is usually operated in this temperature range.

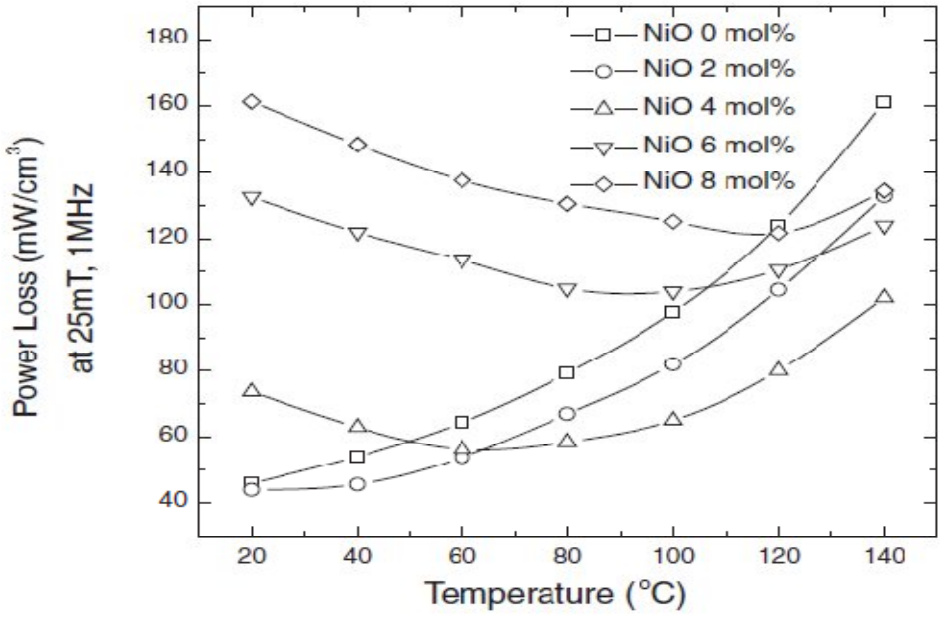

Figure 2.7 the temperature dependence of the power loss at 25mT and 1MHz for various NiO contents.

The present day research activity has been concentrated on high-frequency and low loss materials for the development of switching mode power supplies (SMPS) at higher temperatures [15]. In SMPS, the power increases with an increase of switching frequency. There were many efforts to make SMPS more compact and to increase their operating frequency up to megahertz range. Microwave–Hydrothermal (M–H) method has been successfully used for the synthesis of nanocrystal- line Mn–Zn ferrites which are used for high-frequency applications. As-synthesized powders were characterized using X-ray diffraction (XRD) and transmission electron microscopy (TEM).

Y.H. Han et al [16]. In their study mentioned that the sintering temperature significantly changed the microstmcture and affected the power loss behavior at the frequency range over 100kHz. The best power loss characteristics at 100 kHz-200mT and 500 kHz-50mT were obsemed in the samples sintered at 1300°C and 125O^{o}C, respectively. Those results

indicated that the power loss depended on the grain size, electrical resistivity and density of sintered cores. To maintain the stoichiometries at the sintering condition, the ferrite cores were processed on the isocomposition lines within the spine1 phase boundary when being cooled. The zinc vapor pressure as well as the oxygen partial pressure was controlled. The high zinc loss condition had an adverse effect on the microstructure of the sintered core surface and degraded the power loss characteristics.

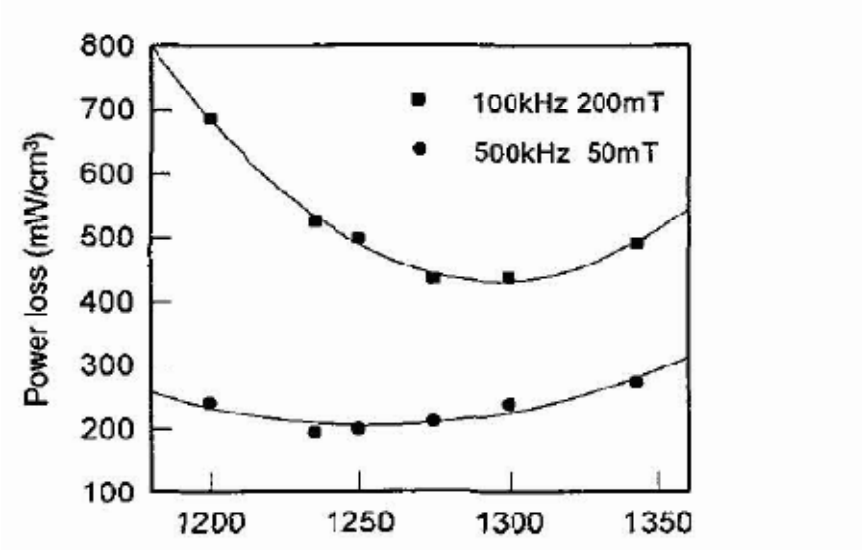

Figure 2.8 Effect of sintering temperature on power loss at 100 kHz, 500 kHz and 8O°C.

The power loss of Mn-Zn ferrites consists of hysteresis loss and eddy current loss for the power applications. The eddy current loss is considered a more important loss characteristic for the high frequency applications, which is proportional to d^2/p where d and p represent grain size and resistivity, respectively.

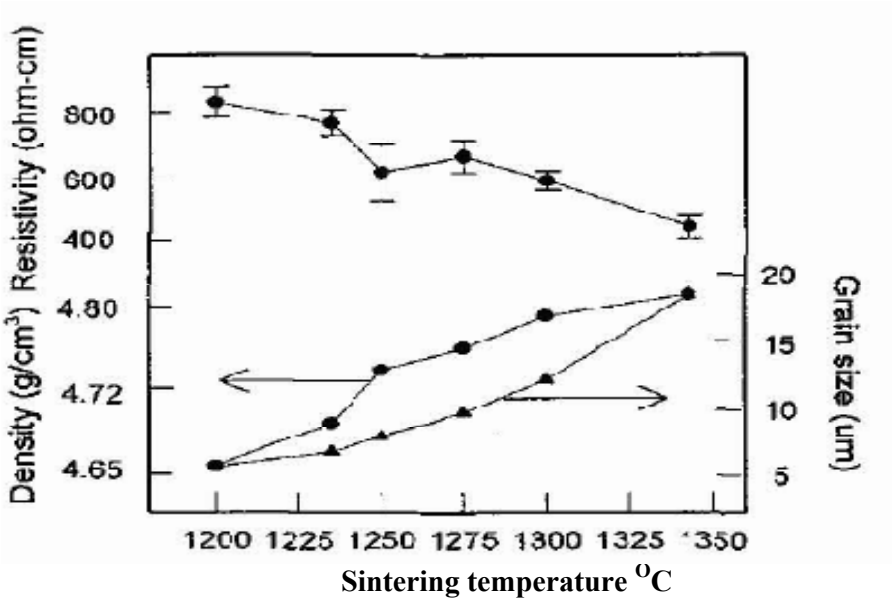

Figure 2.9 Effect of sintering temperature on resistivity, density and grain size.

In 2005 Ratnamala Chatterjee & Anjali Verma worked on Development of a new soft ferrite core for power applications **[17]**. Manganese-substituted nickel–zinc ferrites have been investigated as power core materials for applications in switched-mode-power supplies. High frequency operation of these power supplies requires high performance cores with low power losses. The main contributors to the power loss are eddy current loss, hysteresis loss and residual loss. The ferrites have been synthesized by the citrate precursor technique and their electromagnetic properties such as resistivity, permeability, saturation magnetization and Curie temperature studied. A power loss of 500 mW/cc could be obtained at a frequency of 500 kHz, flux density of 50mT and temperature 100^0C.

The main types of losses encountered in ferrites are the eddy current loss, hysteresis loss and residual loss. Consequently the requirements of a power ferrite are high resistivity to keep the eddy current losses low, high permeability to reduce hysteresis losses and a high resonance frequency to reduce the residual losses, which consist mainly of resonance-relaxation losses.

The main method usually adopted to improve the resistivity of Mn–Zn ferrites is the use of certain additives such as CaO and SiO_2 which segregate at the grain boundaries rendering them insulating. Although this method improves resistivity, it may result in reduction of permeability and increase of hysteresis loss.

X-ray diffraction analysis revealed that the samples crystallized in the single-phase cubic spinel structure. The X-ray diffractogram obtained for $Mn_{0.2}Ni_{0.3}Zn_{0.5}Fe_2O_4$ powder calcined at 500 ^{0}C is shown in Fig.2.10. The (h k l) values corresponding to the diffraction peaks are marked in the figure. The broadness of the peaks indicates the fine crystalline nature of the powder. The lattice parameters 'a' for the sintered samples calculated from the (3 1 1) diffraction peak, are shown in Table 2.2. The increase in the value of 'a' with increase in Mn substitution can be understood in terms of the ionic radii of Mn and Ni ions. Because the ionic radius of Mn, 0.91Å, is higher than that of Ni, 0.78Å, the increase in the lattice parameter with increase in Mn concentration is expected.

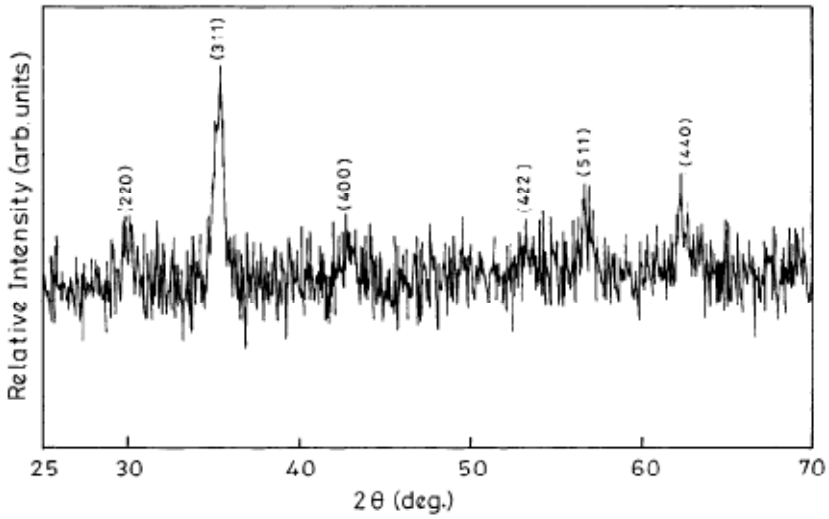

Figure 2.10 X-ray diffractogram of $Mn_{0.2}Ni_{0.3}Zn_{0.5}Fe_2O_4$ powder calcined at 500 ^{0}C [17].

Table-2.2

Lattice parameter a for $Mn_xNi_{o.5-x}Zn_{0.5}Fe_2o_4$ [17]

Ferrite composition x	Lattice parameter, a(Å)
0.1	8.365
0.2	8.384
0.3	8.398

Table 2.3

Properties of $Mn_xNi_{o.5-x}Zn_{0.5}Fe_2o_4$ ferrites [17]

Ferrite composition x	ρ (Ωcm)	T_c (^{o}c)	μ_i
0.1	6.4×10^4	322	400
0.2	1.2×10^4	323	885
0.3	8.9×10^3	312	180

A look at the initial magnetic permeability, μ_i, of the ferrites in Table 2.3 shows that the composition with x = 0.2 exhibits the highest value of permeability. The reported initial permeability of $Ni_{0.5}Zn_{0.5}$ ferrites is 250, while that for $Mn_{0.5}Zn_{0.5}$ ferrites is 1700.

The permeability is greatly dependent on the chemical composition of the ferrite, especially the zinc content. Hence the choice of the chemical composition of the ferrite is crucial. The ferrite with 50 mol% of zinc is found to exhibit the highest permeability at room temperature and hence compositions with zinc 50 mol% were chosen for the preparation of power ferrite cores.

In 1999 A. Znidarsic and M. Drofenik [18] investigated the microstructural development and magnetic properties of Mn-Zn ferrites doped with various amounts of CaO and sintered in atmospheres containing various oxygen concentrations. They indicated the strong link among the amount of CaO segregated in the grain boundaries, oxygen concentration during sintering, average grain size and the magnetic properties of the Mn-Zn ferrites. CaO in Mn-Zn ferrites together with low oxygen partial pressure during sintering were recommended for low power loss due to the decreased average grain size, increased grain boundary resistance and high density.

Zaspalis et al. [19] in 2002 worked via grain boundary engineering to modify the magnetic properties of Manganese Zinc ferrites. They investigated the effect of Nb_2O_5 addition on the power loss properties of Mn-Zn ferrites. They proposed that Nb_2O_5, when added in quantities up to 200 PPM, acts as a local grain boundary oxidizing agent that inhibits grain boundary zinc evaporation and therefore helps reducing lattice mismatch and associated residual stresses. The Nb_2O_5 associates with the Ca, creating high electrical resistivity grain boundary phases. They suggested almost 17% improvement of the total power losses that is believed partly due to the reduction of the magnetostriction,

stress related hysteresis losses, and partly due to the reduction of the electrical resistivity related eddy current losses.

Topfer et.al [20] studied the microstructural effect in low power loss ferrites by the addition of various dopants and concluded that the microstructure of the ferrite is determined by a variety of factors such as, raw material quality, Calcination temperature, milling procedure and sintering regime. Moreover, the concentration of dopants and impurities effectively regulates the densification process and the grain boundary properties. The effect of CaO and SiO_2 on the microstructure and magnetic properties was studied intensively. SnO_2 and Nb_2O_5 were proposed as an additive, which gets dissolved in the ferrite grains or segregate at grain boundaries and reduce losses. They also correlated the magnetic losses with the sintering temperature and additive concentration.

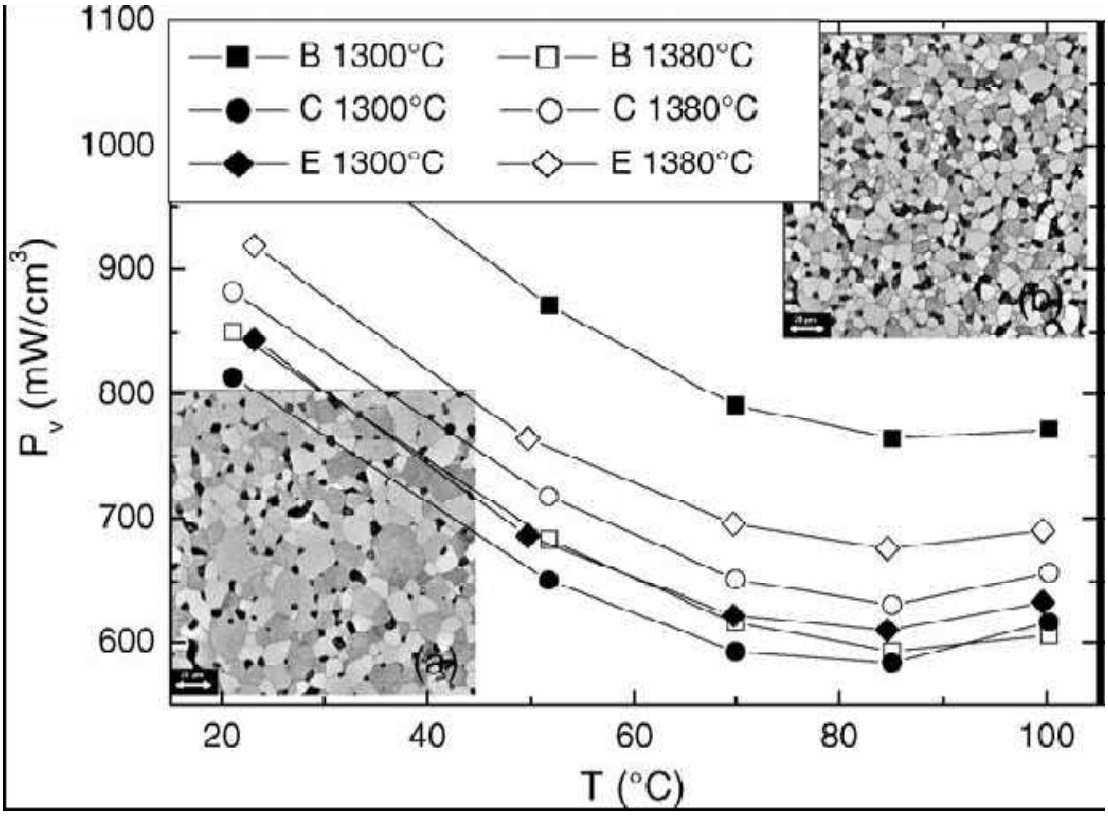

Figure 2.11 Power loss at 100 kHz and 200mT as function of temperature for samples with CaO and SiO_2 addition (B) and with SnO_2 (C) and Nb_2O_5 (E).Inset: SEM micrographs of samples B sintered at 1380 ^{o} C (a) and 1300 ^{o} C (b) [19].

B. Parvatheeswara Rao et al [21] have studied the dielectric loss tangent of Mn-Zn ferrite materials. These have been prepared by conventional ceramic technique to investigate and understand the influence of pentavalent niobium additions on the dielectric behavior of Mn-Zn ferrites as a function of composition and frequency. Dielectric constants of these ferrites have been found to be of the order of 10^6. The dielectric loss has been found to be smaller for the samples containing niobium. Additions of pentavalent ions in Mn-Zn ferrites have been reported to improve the core losses.

The variation of tan delta versus frequency for the sample doped with 0.3 wt% Nb_2O_5 is shown in Fig. 2.12. The dielectric loss is minimal up to 2 MHz and thereafter it increases and exhibits a peak at 4 MHz all the samples show similar dielectric loss peaks in the MHz region.

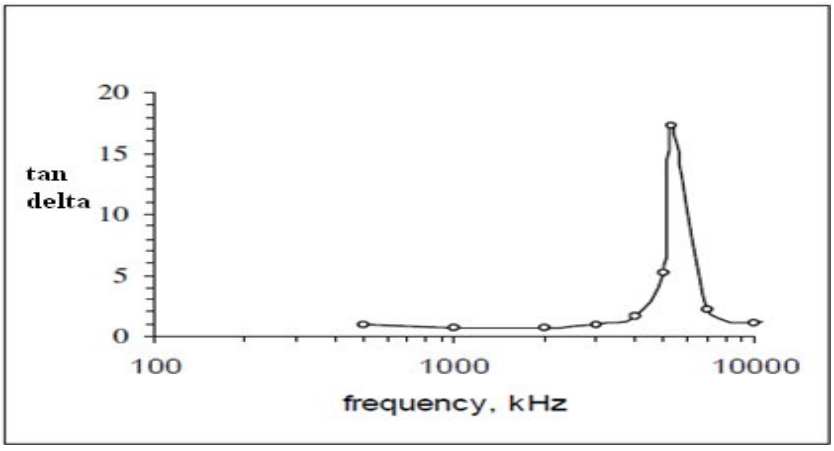

Figure 2.12 Variation of dielectric loss versus frequency for the sample added with 0.3 wt% $Nb_2 O_5$.

Aim of the work

Low power loss material is an excellent solution for many circuit requirements, especially DC-DC converters and high frequency filters. Low power loss material is available in a wide variety of core shapes and sizes up to 25 mm, including planars, PQs, torroids, and other shapes. This material can be shaped to any core design and can be used in the Inverter transformers for LCD backlight, AC adapters and chargers of notebook type PC's.

Aim of the present work is to develop low power loss Mn-Zn ferrite materials for power applications which can be operated at high frequency. Low power loss Mn-Zn ferrite with a permeability of 1000-1100 which can be used in the frequency range of 0.5 to 3 MHz will be suitable one.

CHAPTER 3

EXPERIMENTAL WORK

This chapter highlights the experimental work carried out in different stages of the project, which involves

- Preparation of Ferrite powder and its characterization.
- Forming powder into cores.
- Firing or Sintering.
- Characterization and testing of cores.

3.1 Powder Preparation

The ferrite powders were produced by conventional ceramic processing technique, which is one of the most critical steps that control the electrical and magnetic properties of the finally obtained ferrite cores. It consisted of following steps:

3.1.1 Dry Mixing

High purity raw materials of the basic composition 52.50 mole% ferric oxide (99.8% purity), 41.20 mole% manganese oxide (92% purity) and remaining 6.30 mole% zinc oxide (99.4% purity), were mixed and blended homogenously through dry mixing in the pot mill for few hours.

3.1.2 Calcination

The mixed oxides are calcined at temperature 950°C for 90 minutes in air atmosphere in the batch type furnace. The purpose of calcining is to start the process of forming of spinel ferrite lattice. This process is essentially one of inter-diffusing phenomenon of substituent oxides into a chemically and crystallographically uniform structure. The driving force for the interdiffusion is the temperature and concentration gradient. As the individual oxides inter-diffuse, some ferrite is created at the interface. This complete phase reduces further diffusion because the concentration gradient is no longer present to act as a driving force. The material in the centre of each oxide particles remains as such, as they experience the difficulty in diffusing through the ferrite since the diffusion distance becomes larger. Since some shrinkage occurs in calcining, one advantage of the

process is to reduce the shrinkage in the final sintering. This allows better control of the final dimension of the sintered core. In addition, calcining helps in evaporation of the volatile impurities and homogenization of the powder mixture.

During this process, the powder coarsens considerably, and the colour changes from red to grey or black. The degree of calcining action, or in other words spinel formation can be studied from the X-ray Diffraction (XRD) pattern. It shows the peaks of spinel phase formed and the unreacted residual Fe_2O_3 or hematite phase.

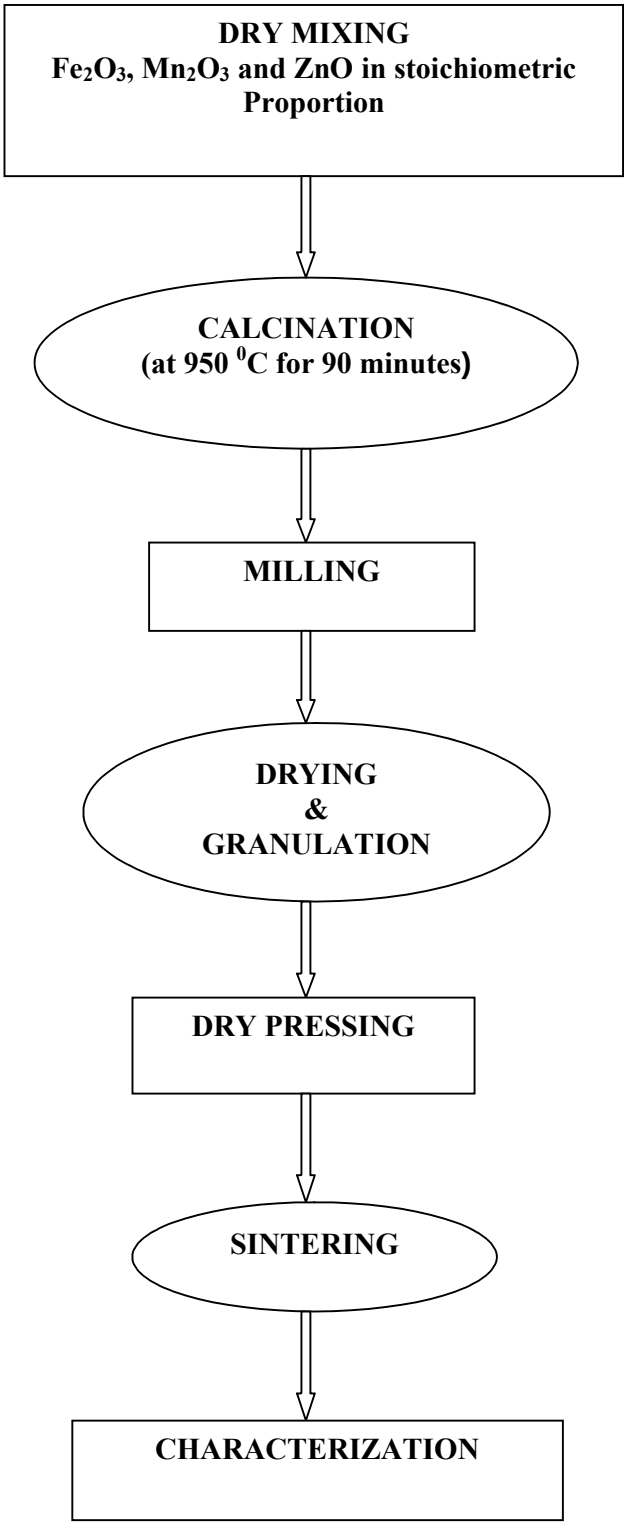

Figure 3.1 Flow sheet for the synthesis of sintered Manganese Zinc Ferrites.

3.1.3 Milling

After calcining, the material is broken up by ball milling and attrition action. The particle size reduction is carried out to achieve the desired specific surface area (SSA) of 4700 cm^2/gm through ball milling with 32 mm steel balls followed by fine milling in attritor with 6 mm steel balls. The amount of milling determine the particle size distribution, which in turn influence the homogeneity of the compact going into the final firing as well as the microstructure after the sintering process. In the mid-stage of milling, high purity additives such as niobium oxide, calcium oxide, zirconium oxide etc in desired quantity are added to the slurry in the ball mill. Specific surface area (SSA) is measured through Blains apparatus.

In this project a total of six samples were prepared with the same basic composition of 52.5 mole% ferric oxide, 41.2 mole% manganese oxide and 6.3 mole% zinc oxide and fixed amount and type of dopants, only variation in NiO dopants are present in the prepared samples. The composition, dopants level and types are mentioned in the table 3.1. Variation in the properties of the finally sintered ferrite cores with the amount and type of dopants were studied.

Table 3.1 Composition of dopants.

Sample No.	CaO (PPM)	ZrO_2 (PPM)	Nb_2O_5 (PPM)	NiO (PPM)
1	500	200	200	NIL
2	500	200	200	200
3	500	200	200	500
4	500	200	200	1000
5	500	200	300	NIL
6	500	200	200	NIL

3.1.4 Drying and Granulation

Slurry obtained after milling is then dried in the oven, so as to remove the moisture and obtain a press-able powder. Organic additives such as Polyvinyl Acetate (PVA) and. Polyethylene glycol (PEG) are employed to facilitate this step. PVA is added as a binder to provide adequate green strength to the pressed compact, so that it can be handled easily in the green stage for further processing, PEG acts as a plasticizer so as to soften the particles [21].The mixture of PVA, PEG and dried slurry is than granulated in the agate mortar, so as to obtain free flowing granulates. The granules are classified by mechanical sieving and the fraction between 200 and 500 Vm are subsequently used for pressing.

3.2 Forming

The second step in the ferrite processing technology is the forming of the components. In this step, dry pressing of granulates into the torroid core configuration is carried out. Dry pressing or compacting is done in a mechanical press using a combined action of top and bottom punches in a cavity such that torroids of external diameter of 29.13 to 29.20 mm, internal diameter of 17.38 to 17.45 mm and height of 14.17 to 14.25 mm is obtained. In this process torroid cores with the green density of 3 to 3.2 gm/mm^3 are obtained.

Figure 3.2 below shows some of the aspects of die pressing.

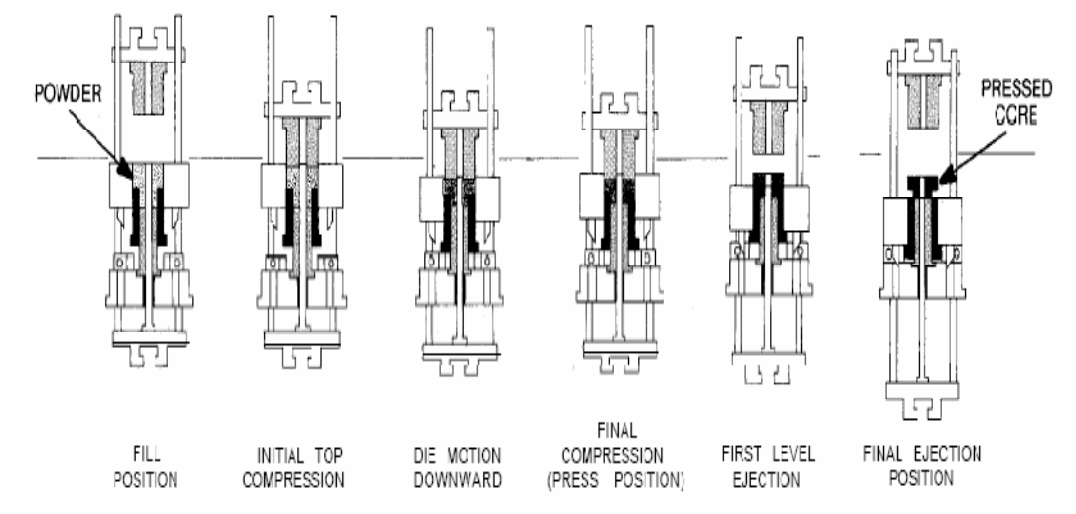

Figure 3.2 Dry pressing techniques.

Before proceeding for dry pressing, granulates are treated with external lubricants such as zinc stearate, which produces a coating of fine lubricant particles on granule surface, External lubricants also serve to lubricate the die and punch surfaces. The addition of external lubricant increases tool life and helps produce a uniform green body. In addition to providing die-wall lubrication, external lubricants can improve the flow properties of granulated powder by reducing inter-granular friction and hence fill the die more efficiently. Improved packing characteristics can eliminate large inter-granular voids and hence contribute to a low porosity microstructure of the final sintered ferrite core.

3.3 Sintering

This is the most critical step in the ferrite processing. It is during this phase of the process that the product achieves its final electric, magnetic and mechanical characteristics. Sintering of manganese-zinc ferrites requires equilibrium between time, temperature and atmosphere along each step of the sintering cycle. Sintering starts with a gradual ramping up from room temperature to approximately 900 ^{o}C as impurities, residual moisture, binders (PVA, PEG), and lubricants (Zinc stearate) are burned out of the product. The atmosphere in this part of the sintering cycle is 20% oxygen (complete air).

The temperature is further increased to the final sinter temperature of 1320 ^{o}C at high heating rate. While the temperature is increasing, nitrogen gas is introduced into the kiln and the partial pressure of oxygen is maintained at 5% at the sintering temperature of the kiln atmosphere. During the cool-down cycle a reduction of oxygen pressure is very critical in obtaining high quality Mn-Zn ferrites and so the oxygen partial pressure is dropped down to ppm level. Sintering of the green torroid samples is carried out in programmable Linn batch kiln. Firing schedules and equilibrium oxygen partial pressure conditions maintained are indicated in the sintering profile in the table 3.1.

Figure 3.3 shows the typical sintering profile carried out in this project.

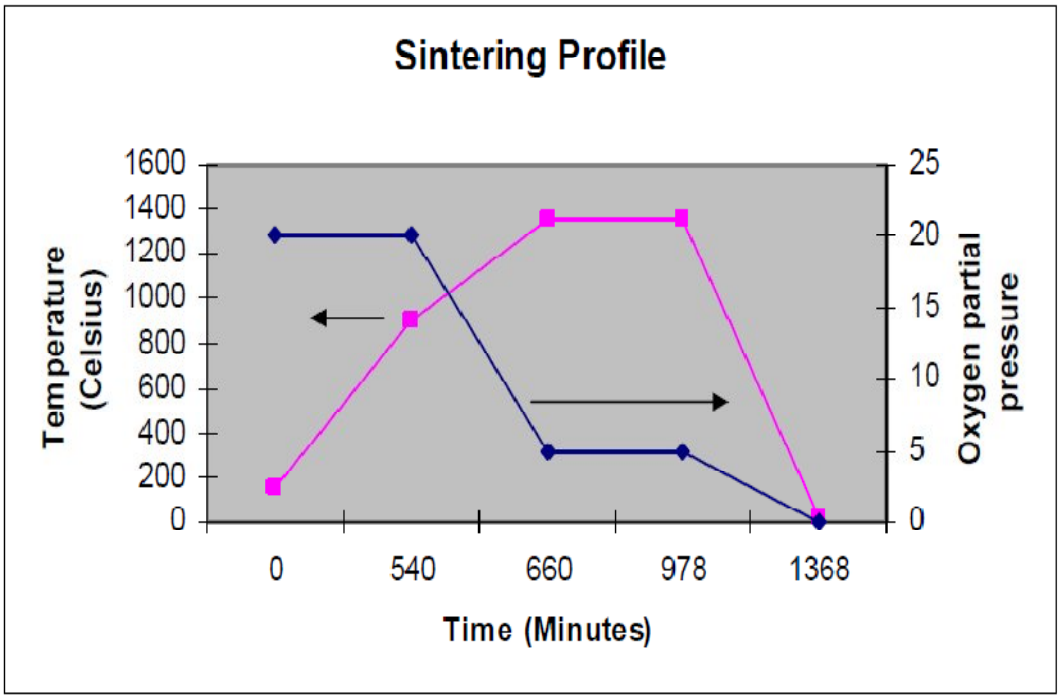

Figure 3.3 Schematic Diagram of the atmosphere and temperature profiles used during sintering.

Table 3.2 Typical Sintering Profile.

Sintering profile			
Time Hrs	**Time (Min)**	**Temp (^{o}c)**	**Oxygen (%)**
0	0	150	20
9	540	900	20
11	660	1320	5
15.3	978	1320	5
22.8	1368	25	0.01

Table 3.3 Dimensions, volume and Density of the sintered MnZn ferrite torroid samples.

Sample no.	Outer Diameter [D_1] (mm)	Inner Diameter [D_2] (mm)	Height [h] (mm)	Weight [gms]	Volume (cc)	Density [gm/cc]
1	25.24	15.20	11.93	17.43	3569	4.57
1	25.18	15.12	12.00	17.56	3582	4.58
2	25.08	15.09	11.99	17.43	3544	4.59
2	25.06	15.08	12.08	17.43	3565	4.56
3	25.13	15.07	11.99	17.60	3569	4.60
3	25.08	15.06	12.13	17.60	3592	4.58
4	25.18	15.13	11.96	17.46	3568	4.57
4	25.19	15.06	11.98	17.47	3592	4.47
5	24.93	15.02	12.18	17.62	3553	4.63
5	25.03	15.05	11.99	17.57	3532	4.64
6	24.67	14.88	12.16	17.83	3470	4.73
6	24.66	14.90	12.18	17.87	3472	4.82

3.4 Characterization

3.4.1 Electrical and Magnetic Characterization

Detailed studies of the electromagnetic properties of ferrite samples were carried out. The type of measurement of samples is mansion fallowing steps.

1-Power Loss (P_v) measurement

2-Magnetic Flux Density (Bmax) measurement

3-Inductance Factor (A_L) measurement

4-initial permeability (μ_i) measurement

5-Magnetic Saturation (Bsat) measurement

6- Curie Temperature (Tc) measurement

7-Dielectric Loss Tangent measurement

The measurement of Inductance factor (A_L) and Inductance (L_S) of each sintered torroid was carried out using Hewlett Packard multi-frequency LCR meter (model no.-4275A), and other properties such as initial permeability, were derived using the mathematical relations mentioned in the literature. Inductance Factor A_L (nH), which is the inductance of the coil on the specified core divided by the square of the number of turns, was directly measured through LCR meter under test conditions, of frequency of 10 KHz and voltage of 150mV, by putting the probes at the centre of each torroid sample. The resistance of the ferrite core was measured by putting the probes of the multi-meter at the two specific points on the ferrite core.

For measuring the Inductance value, the torroid samples were properly wound with the copper wire with 20 turns and the measurements were carried out using LCR meter at the test conditions of frequency set at 10 KHz and voltage of 0.005 Volts. Initial permeability (μ_i) of of the torroid samples with 20 turns in the coil were calculated using the inductance value in the below mentioned mathematical relation [20].

$$\mu_I = [4\pi Ls/ h \ln (D_1/D_2)]$$

Where h represents the width of the core, D1 and D2 are outer and inner diameters of the torroid core respectively.

Variation of initial permeability with temperature was studied using the Curie set up consisting of a wound ferrite sample dipped in the silicon oil containing flask placed over a heater. The ferrite core is uniformly heated at a constant heating rate and the Inductance value corresponding to the temperature is measured by LCR meter. Initial permeability was calculated according to above equation and its value is plotted against temperature. Due to the limitations of the available apparatus, Curie temperature of the samples was not measured. Variation in Initial permeability with frequency is measured similarly through LCR meter and plotted.

Power loss characteristics and magnetic flux density B_{max} of the ferrite samples were studied using power loss analysis set up consisting of Signal generator (Model-FG2002C), Power amplifier (Model no.-EV- 300/F) and Norma AC/DC Power analyzer (Model no.-D5245). Power loss was measured under the conditions of 50 KHz /100 mT,

100 KHz /50mT, 100 KHz/100 mT, 100 KHz/200 mT and 200 KHz/100 mT, B_{max} was measured at the frequency 16 KHz, and magnetic field of 250 Amp/m. Variation in power loss and B_{max} with temperature was studied by placing the test samples in the dry heating chamber. Temperature in the heating chamber was varied by the interval of 25 ^{0}C up to 120 ^{0}C and corresponding variation in above mentioned properties was measured.

The dielectric loss measurements are made using HP 4294A Impedance Analyzer. Variation of dielectric loss tangent (tan δ) determined at 500 KHz to 3 MHz.

Saturation magnetization (Bsat) measurements were performed at 10 KHz, and magnetic field 1000 Amp/m. The measurement conditions of sample at 25^{o}C and 100^{o}C.

CHAPTER 4

RESULTS AND DISCUSSION

The synthesized ferrite powders and sintered ferrite samples were characterized following the procedure mentioned in Chapter-3. Before doing instrumental characterization, powders were visually inspected. Spinel powders were dark grayish/blackish in color. When brought nearer to a permanent magnet, they were strongly attracted to the magnet, suggesting ferrite formation. In this chapter, results obtained from the characterizations are discussed.

4.1 Electrical and Magnetic properties

Manganese Zinc ferrite samples synthesized in this work were tested for their electrical and magnetic properties. The outcome of the electrical and magnetic characterization of the samples is discussed in the following paragraphs.

4.1.1 Power Loss Characteristics

Power loss density (Pv) and magnetic flux density (B_{max}) of the ferrite samples were measured through power loss set up as mentioned in the preceding chapter. Power loss was measured under the conditions of 50 KHz /100 mT, 100 KHz /50mT, 100 KHz/100 mT, 100 KHz/200 mT and 200 KHz/100 mT for each sample, Magnetic flux density B_{max} was measured at the frequency of 16 kHz and magnetic field strength of 250 A/m. The values of the measured properties are mentioned in table 4.1. The power loss variation with temperature is shown in the following table.

Table 4.1 Measured values of power loss of Mn-Zn ferrite samples at 50 KHz /100 mT.

Temp.°C	Sample-1	Sample-2	Sample-3	Sample-4	Sample-5	Sample-6
25	106	106	109	110	119	54
40	96	97	101	103	114	45
60	72	57	73	75	83	33
80	56	57	58	59	68	28
100	41	40	44	45	52	35
120	30	30	31	33	40	31

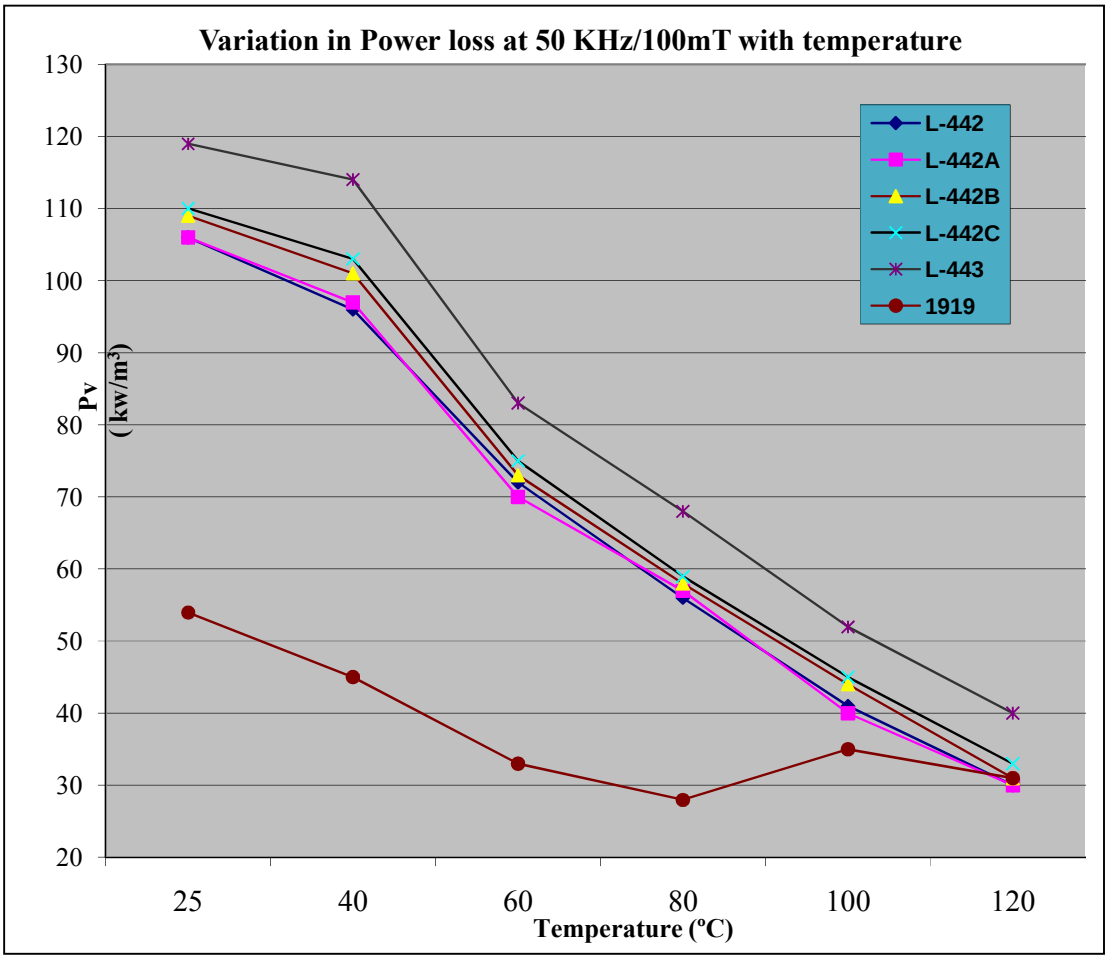

Figure 4.1 Variation in power loss of Mn-Zn ferrite samples with temperature at 50 KHz/100mT

Table 4.2 Measured values of power loss of Mn-Zn ferrite samples at 100 KHz /50 mT.

Temp.^{o}C	Sample-1	Sample-2	Sample-3	Sample-4	Sample-5	Sample-6
25	49	51	51	50	54	24
40	45	44	46	48	49	23
60	33	33	35	35	38	13
80	27	27	28	29	33	12
100	19	19	19	21	25	11
120	12	12	13	13	18	12

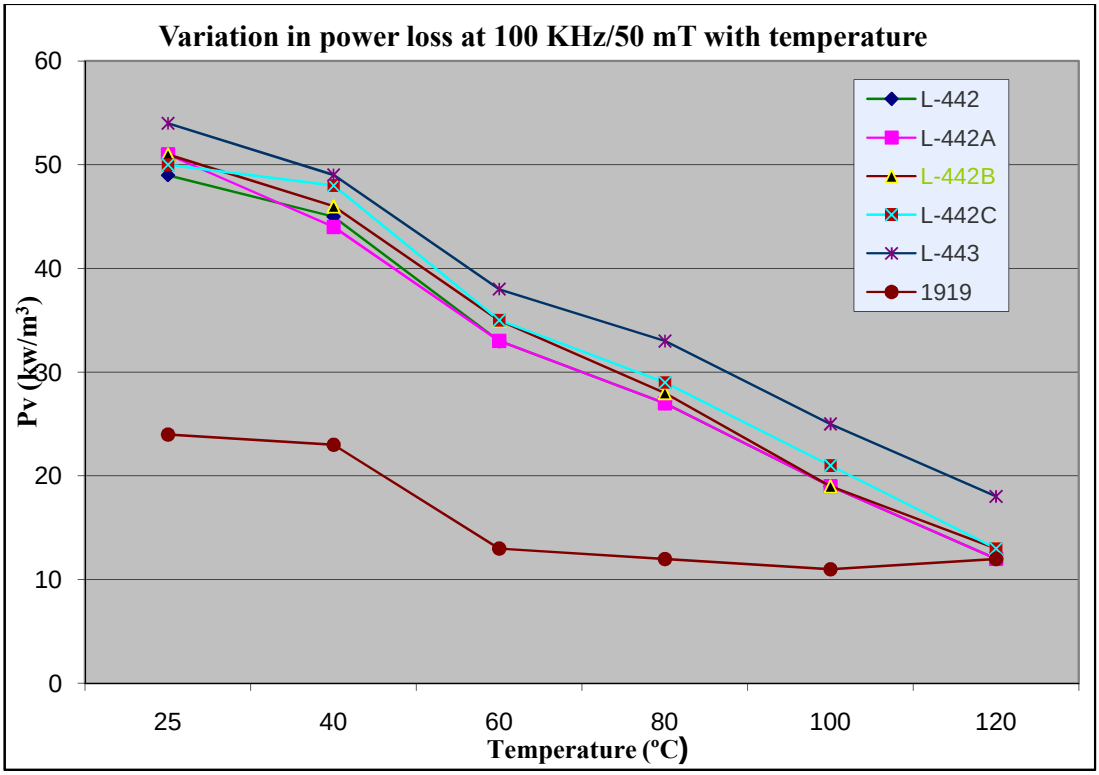

Figure 4.2 Variation in power loss of Mn-Zn ferrite samples with temperature at 100 KHz/50mT

Table 4.3 Measured values of power loss of Mn-Zn ferrite samples at 100 KHz/100 mT.

Temp.°C	Sample-1	Sample-2	Sample-3	Sample-4	Sample-5	Sample-6
25	242	240	246	244	267	129
40	220	223	227	235	257	117
60	171	171	170	175	190	81
80	137	138	139	144	162	74
100	102	103	106	109	125	75
120	79	79	82	85	100	93

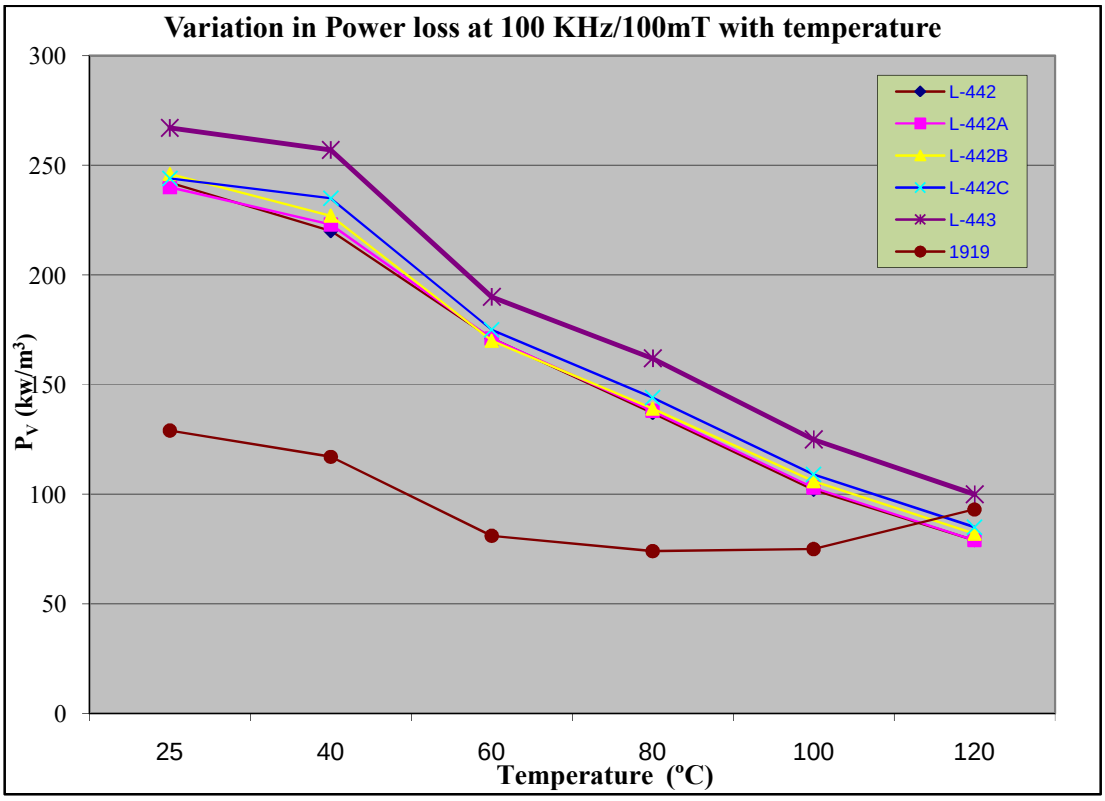

Figure 4.3 Variation in power loss of Mn-Zn ferrite samples with temperature at 100 KHz/100mT

Table 4.4 Measured values of power loss of Mn-Zn ferrite samples at 100 KHz/200 mT.

Temp.^{o}C	Sample-1	Sample-2	Sample-3	Sample-4	Sample-5	Sample-6
25	1063	1040	1037	1060	1147	640
40	949	956	959	1001	1098	592
60	809	803	796	832	907	510
80	679	666	673	695	770	478
100	581	572	565	591	663	526
120	494	490	481	507	565	627

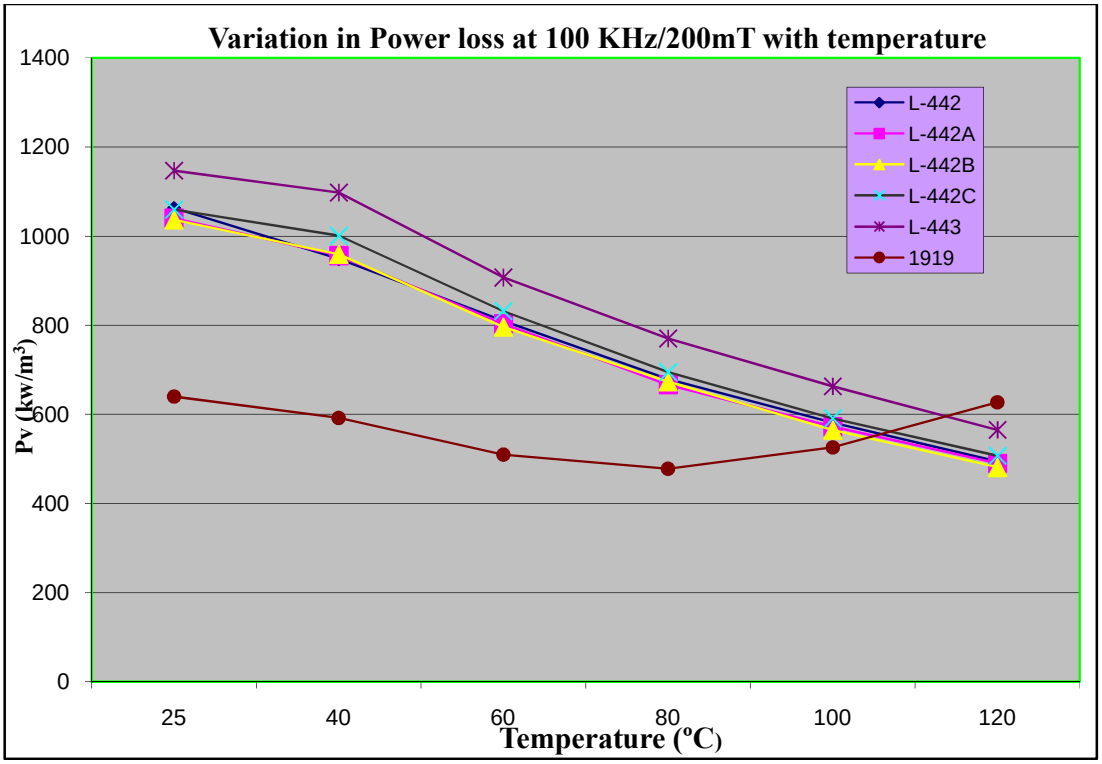

Figure 4.4 Variation in power loss of Mn-Zn ferrite samples with temperature at 100 KHz/200mT

Table 4.5 Measured values of power loss of Mn-Zn ferrite samples at 200 KHz/100 mT.

Temp.^{o}C	Sample-1	Sample-2	Sample-3	Sample-4	Sample-5	Sample-6
25	595	588	592	595	640	354
40	546	559	559	572	617	338
60	458	458	461	478	523	292
80	384	380	380	390	432	263
100	309	309	309	321	361	286
120	260	260	266	273	315	351

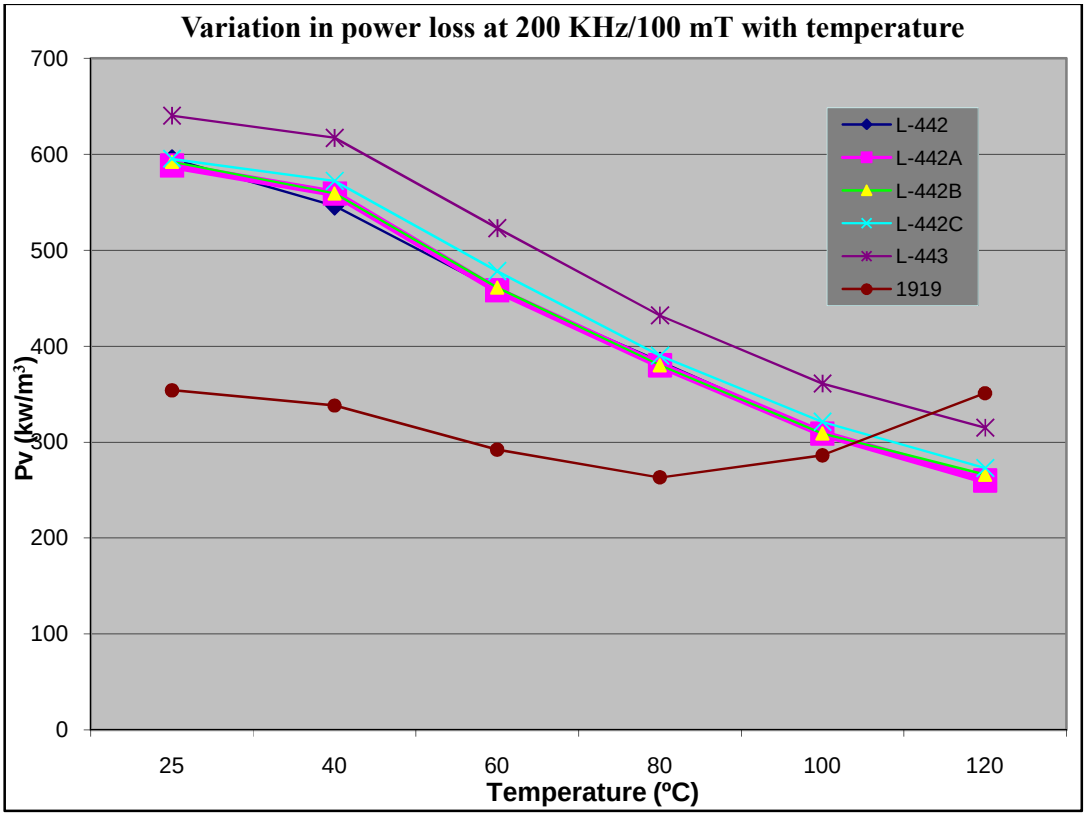

Figure 4.5 Variation in power loss of Mn-Zn ferrite samples with temperature at 200 KHz/100mT

In the fallowing figure 4.6 we have seen that the best power loss properties were observed in the case of sample no. 1 at 200 kHz/100 mT. It means that this sample can work at low power loss at high frequency. The best result of low power loss values are 137 Kw/m^3 at 100 KHz, 80^{0}C and 100 mT, and of 309 Kw/m^3 at 200 KHz, 100^{o}C and 100 mT respectively. The lowest power loss value is reported between 80-120 ^{0}C, MnZn ferrite materials.

The temperature at which the minimum power loss occurs should preferably be about 120^{0}C, because the transformer core is usually operated in this temperature range.

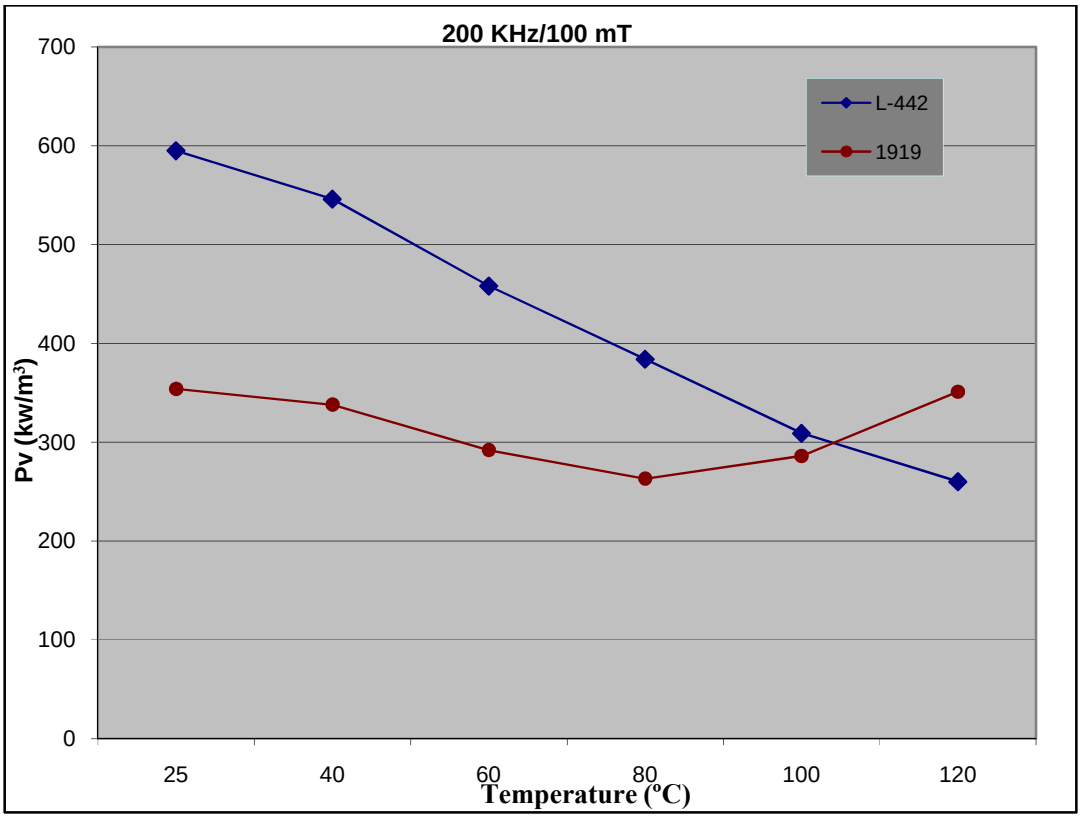

Figure 4.6 Best performance of low power loss of Mn-Zn ferrite samples with temperature at 200 KHz/100 mT.

Addition of CaO leads its segregation at grain boundary which gives highly resistance at grain boundary. Moreover, CaO acts as grain growth inhibiter and gets precipitated at the grain boundary and producing highly resistive grain boundaries. This optimum amount of CaO, ZrO_2 and Nb_2O_5 showing lowest power loss is observed to be 500 PPM,

200PPM and 200 PPM respectively. CaO additions are useful for lowering the ac-conductivity and allow the average grain size minimization.

The reduction in power loss may be attributed to the formation of highly resistive grain boundaries due to the segregation of CaO at the grain boundaries [9]. This exaggerated grain growth annihilates the beneficial influence of CaO on power loss characteristics and produces the negative effect on the initial magnetic permeability of the ferrite samples.

The effect of Zirconium on power loss is not yet clearly mentioned in the literature, but it is known to increase the grain boundary resistivity to a large extent when added along with the traces of Nb_2O_5. It is evident from the measurement of resistance, done by putting the probes of multimeter across the diameter and along the circumference of the torroid samples, that there is a substantial increase in the same with the addition of Nb_2O_5 and ZrO_2. Variation in resistance of the prepared samples is shown in figure 4.7.

Table 4.6 Variation in resistance of the prepared samples.

Sample No.	Resistance KΩ
1	45
2	49
3	47
4	36
5	52
6	27

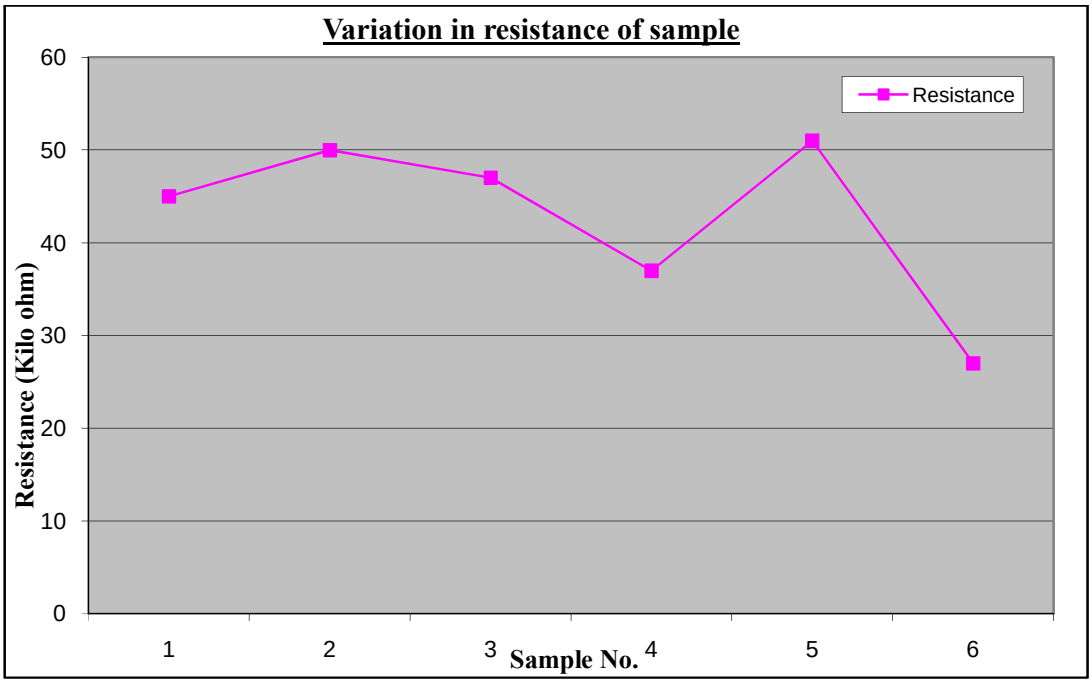

Figure 4.7 Variation in resistance of the prepared Mn-Zn ferrite samples.

The effect of Nb_2O_5 is understood to reduce magnetostriction and stress related hysteresis loss [16] as it acts as a local grain boundary oxidizing agent that inhibits grain boundary Zn evaporation and therefore helps reducing lattice misfit effects and associated residual stresses. Nb atoms get concentrated at the grain boundaries and keep calcium atoms from being incorporated into spinel lattice by pairing Nb^{5+} and Ca^{2+} ions preventing lattice distortion.

4.1.2 Magnetic flux density

Magnetic flux density is the amount of magnetic flux per unit area of a section, perpendicular to the direction of flux. Magnetic flux density (B_{max}) of the ferrite samples were measured through power loss set up as mentioned in the preceding chapter. Variation in magnetic flux density of the samples with temperature measured under the conditions of 16 Khz frequency and applied magnetic field of 250 A/m is plotted in the figure 4.8 below. A slight increase, though random, is observed in the samples with nickel doping.

Table 4.7 Measured values of magnetic flux density for Mn-Zn ferrite samples.

Sample No.	Magnetic flux density [B_{max}] mT 16 KHz/250 A/m	
	25^0C	**100^0C**
1	438	398
2	438	396
3	449	407
4	438	399
5	445	402
6	480	421

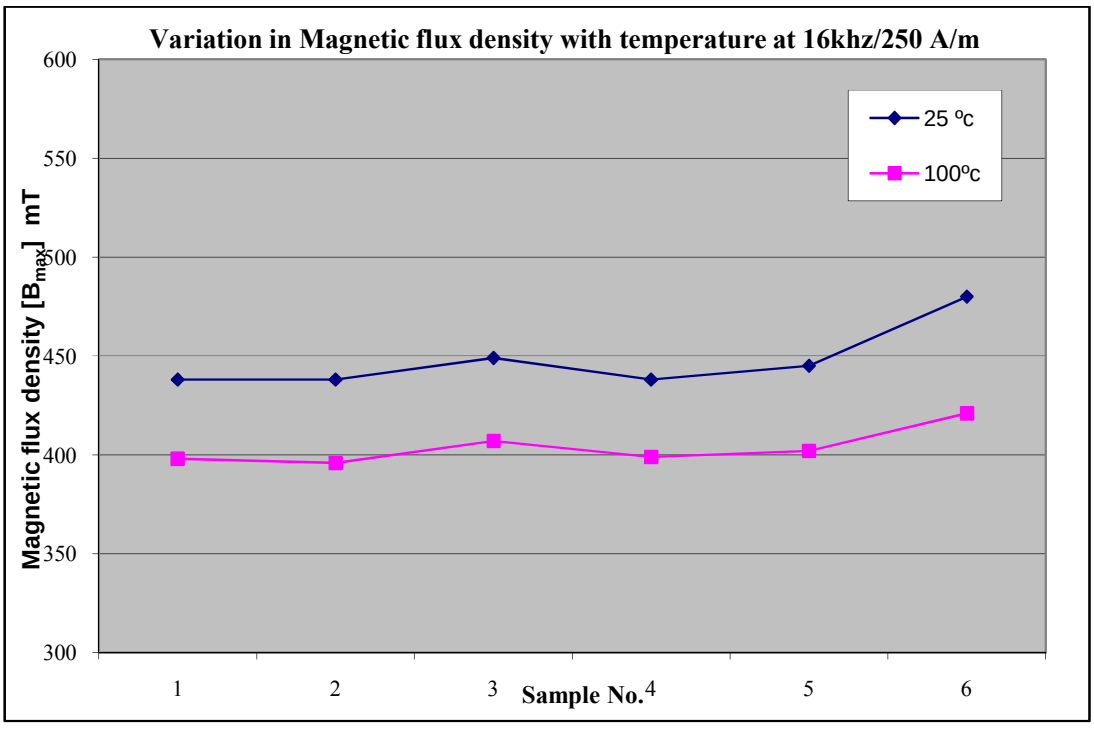

Figure 4.8 Comparative chart of variation of magnetic flux density (B_{max}) with temperature for synthesized Mn-Zn ferrite samples.

4.1.3 Inductance factor, Inductance value and Initial Magnetic Permeability

Inductance factor (A_L), Inductance value (L_S) and Initial permeability of the Mn-Zn ferrite samples prepared in this work measured under the specific conditions discussed in the previous chapters are mentioned in table 4.6.

The initial permeability is greatly dependent on the chemical composition of the ferrite, especially depends on the zinc contents. Hence the choice of the chemical composition of the ferrite is crucial [17].

Table 4.8 Inductance value and Initial permeability of the samples

Sample No.	A_L(nH)	L_s (µH)	μ_i
1	1266	506	1045
2	1253	501	1028
3	1324	530	1070
4	1276	510	1046
5	1270	508	1029
6	2149	860	1748

As revealed by the figure 4.9 below, very high variation is observed in initial permeability of the prepared MnZn ferrite samples as compare to standard sample. The minimum initial permeability result obtained at addition of NiO (200 PPM) as dopants. The initial permeability decreases with NiO content at most of the temperature studied, while addition of NiO increases Curie temperature.

Thus, the decrease in initial permeability is not only due to lower saturation magnetization (M_s) but also to the higher magnetocrystalline anisotropy constants when Ni ions are substituted. Variation is observed in initial permeability and inductance value of the prepared Mn-Zn ferrite samples in above figure 4.10.

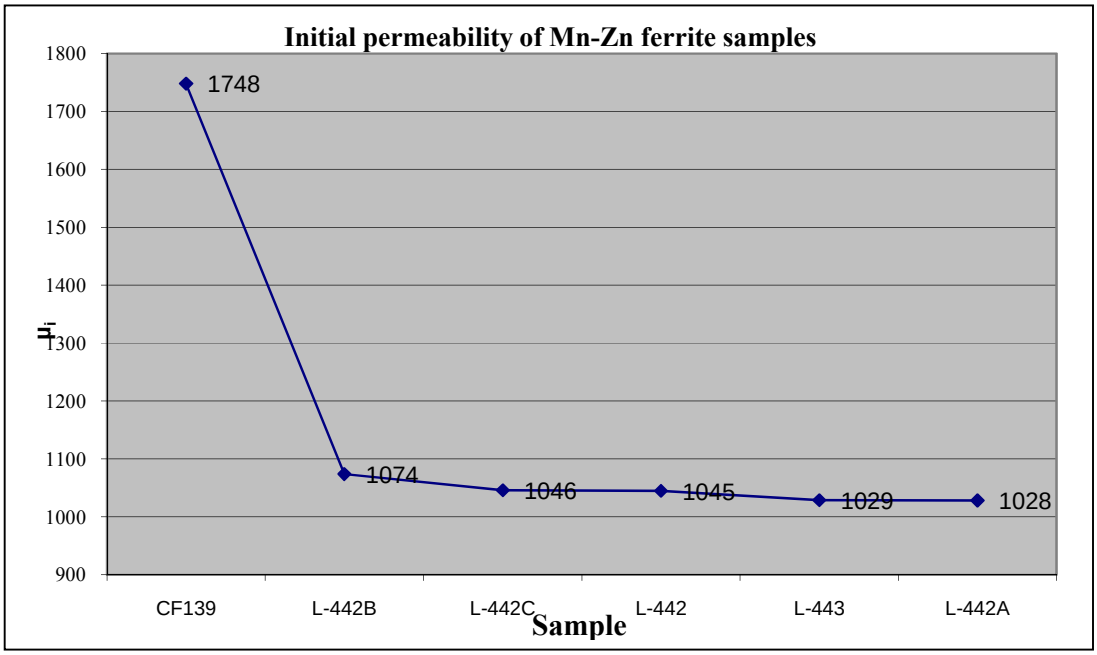

Figure 4.9 Variation in initial permeability of the ferrite samples.

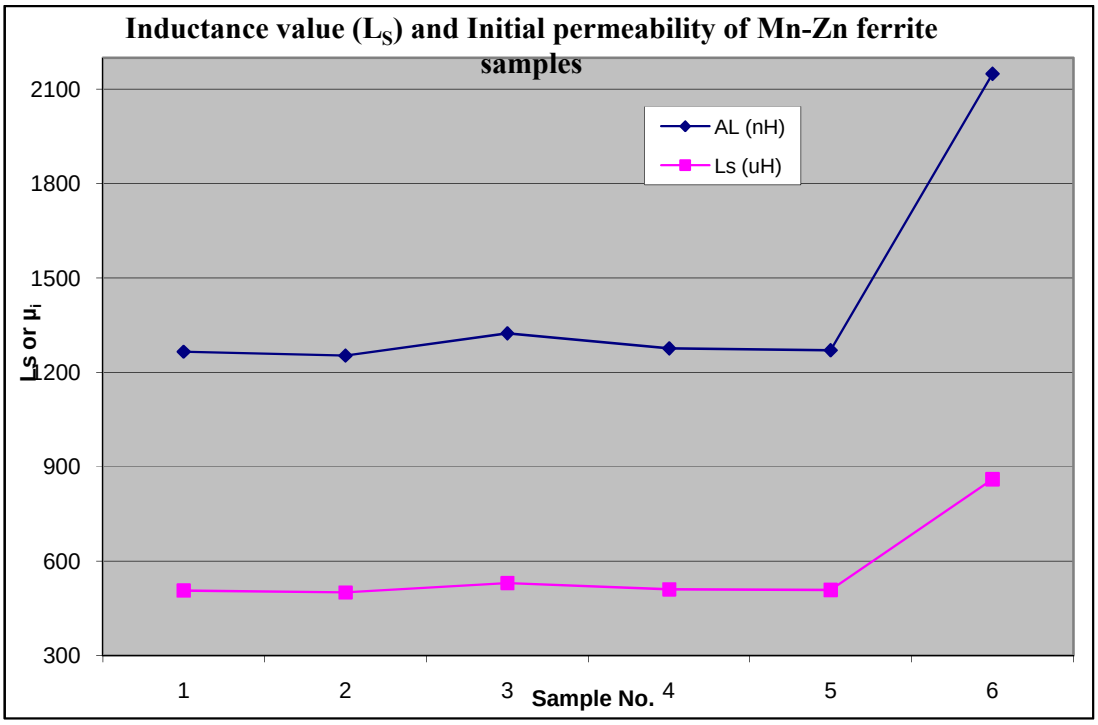

Figure 4.10 Variation in Inductance value and initial permeability of the ferrite samples.

Table 4.9 Variation in Inductance value with Temperature for selected samples at 10 KHz/0.05 volts.

Temperature ^{o}C	Sample-1	Sample-4	Sample-5
28	542	519	504
35	550	528	512
40	605	578	556
50	666	633	603
60	741	710	663
70	797	770	710
80	824	792	733
90	933	891	822
100	1020	984	892
110	1119	1076	980
120	1195	1156	1070
130	1272	1227	1167
140	1298	1286	1242
150	1297	1329	1298
160	1293	1338	1316
170	1247	1338	1425
180	1216	1310	1455
190	1192	1265	1443
200	1182	1256	1437
210	1197	1248	1440
220	1208	1260	1433
230	1236	1254	1430
240	1291	1283	1455
250	1348	1280	1455
260	105	1337	235
270		206	

As revealed in figure 4.11 the Inductance value drops drastically after 260^{o}C. It is the Curie temperature of the samples at which their magnetic properties are lost, hence we can say these ferrite material can be operated up to 260^{0}C. Sample no.1 and sample no.5 have same Curie temperature 260 ^{o}C, while sample no. 4 lost magnetic properties at 270^{o}C. In sample no. 4 NiO used as dopants at 1000 PPM.

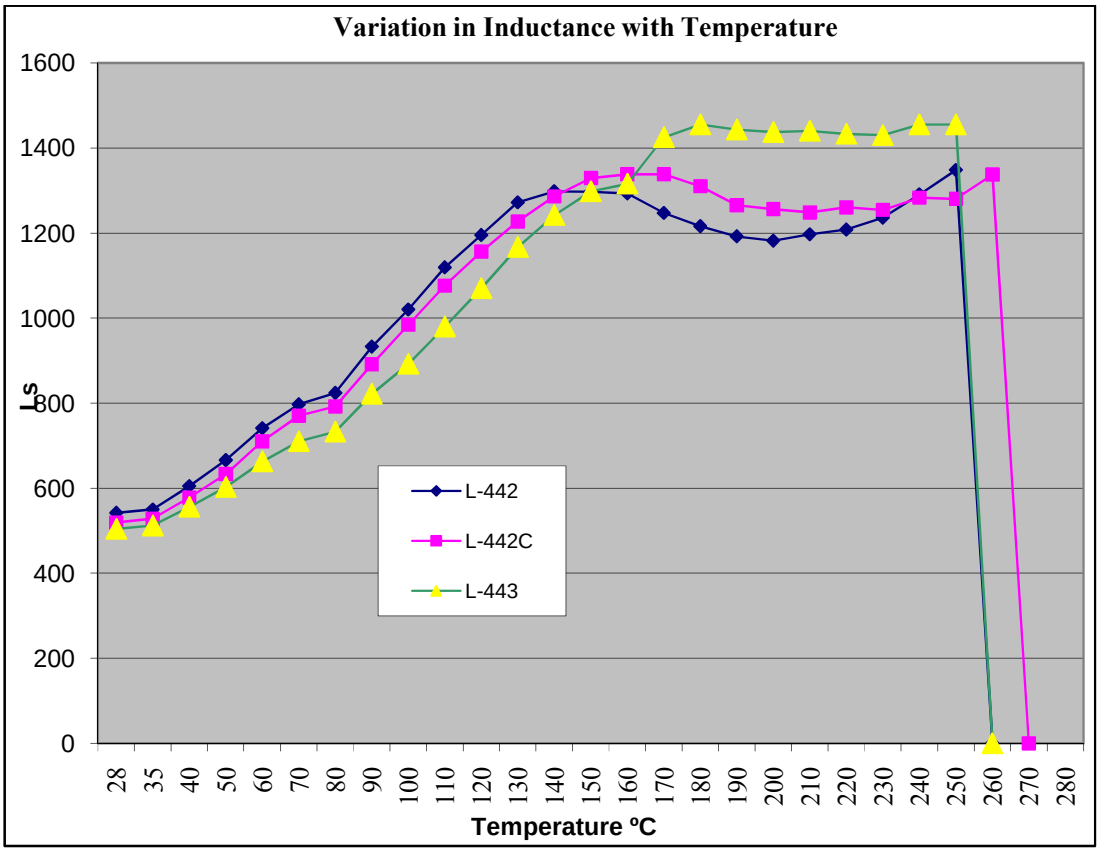

Figure 4.11 Variation in Inductance with Temperature for selected Mn-Zn ferrite Samples.

4.1.4 Magnetic Saturation

Variation in Magnetic Saturation of the samples with temperature measured under the conditions of 10 KHz frequency and applied magnetic field of 1000 A/m is plotted in the figure 4.12 below. The saturation magnetization (Bsat) is observed to be highest at 100 ^{o}C in sample no 1 while at 25 ^{o}C the highest Bsat in sample no.6 (standard sample) and sample no.1. Over all the best magnetic saturation properties seems to be achieved in sample no.1.

Table 4.10 Variation in Inductance with Temperature for selected Mn-Zn ferrite Samples.

Sample No.	**Magnetic Saturation (B_{sat}) 10 KHz/1000A/m**	
	25^0C	**100^0C**
1	486	451
2	479	433
3	487	438
4	478	435
5	481	434
6	523	448

Saturation magnetization depends on the type and the number of ions located at the tetrahedral (A) and octahedral (B) sites in the spinel structure because this distribution affects the magnetization, M_A and M_B of the A and B sub-lattice, respectively. The net magnetization is given as M_B-M_A [17].

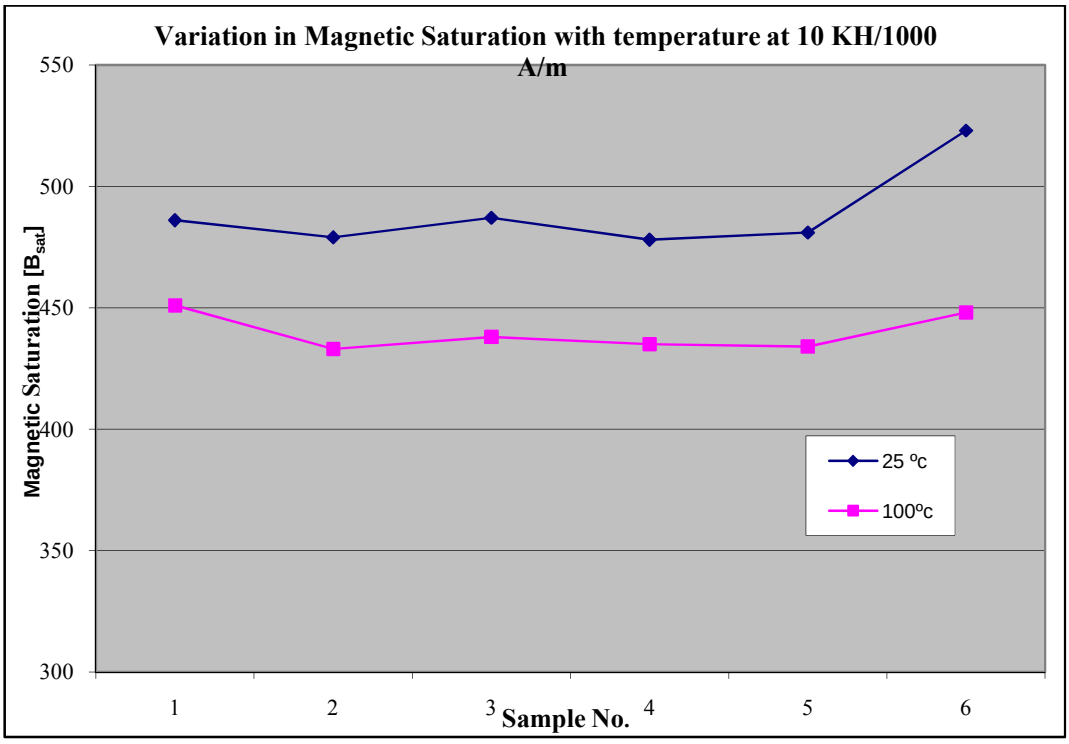

Figure 4.12 Comparative chart of variation of magnetic saturation (B_{sat}) with temperature for synthesized Mn-Zn ferrite samples.

4.1.5 Dielectric Loss

The dependence of the dielectric losses on frequency were studied. Variation of dielectric loss tangent (tan δ) versus frequency is shown in Figure 4.13, 4.14, 4.15, 4.16, 4.17, and figure 4.18 and . The dielectric loss is maximum at 2 MHz in sample no.1,2 3, 4, and sample no.5 while in sample no.6 the maximum dielectric loss obtained at 1 MHz, In figure 4.13 we have seen that peaks obtained at near about 2 MHz frequency range, and in figure 4.14 peaks obtained at 1.2 MHz frequency.

The dielectric loss is maximum is obtained in the sample no 1, 3, 4. Dielectric loss occurs due to the movement or rotation of the atoms. The dielectric behavior in ferrites can be explained on the basis of the assumption that the mechanism of dielectric polarization is similar to that of conduction.

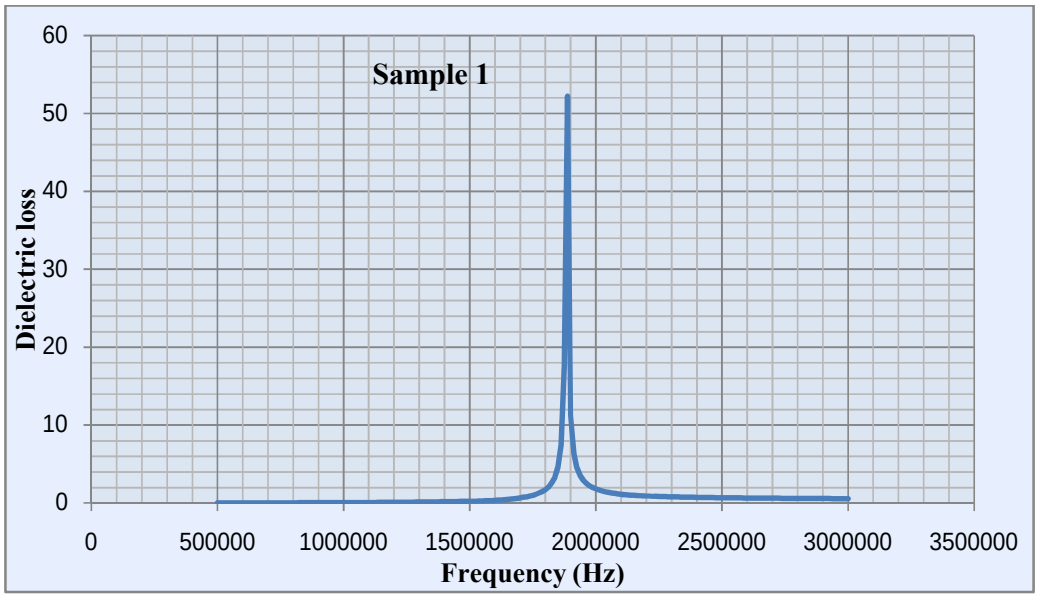

Figure 4.13 Variation of dielectric loss versus frequency for the sample no.1

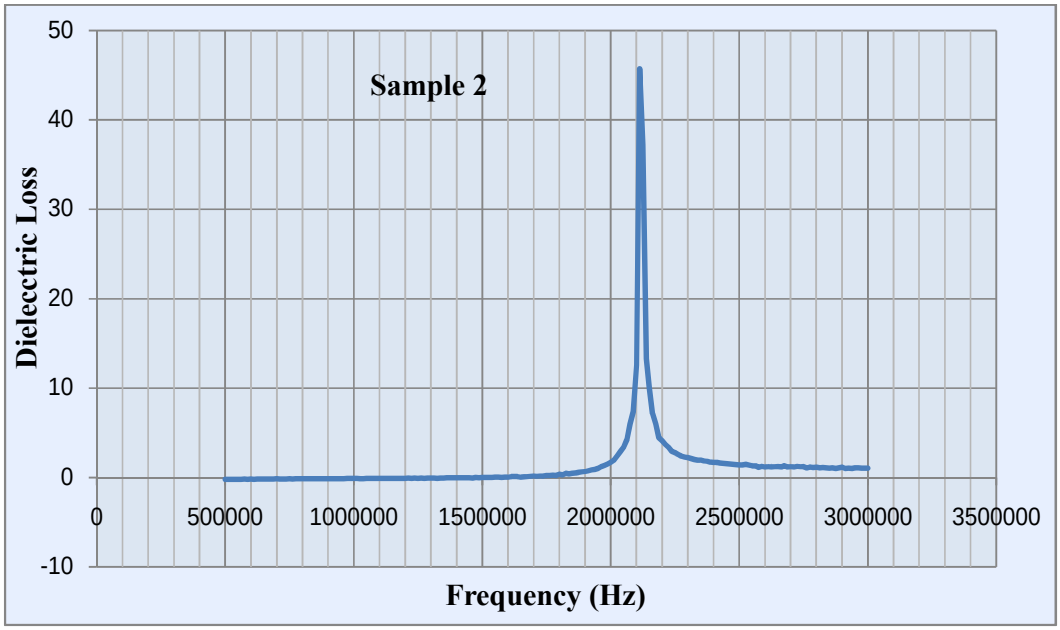

Figure 4.14 Variation of dielectric loss versus frequency for the sample no.2.

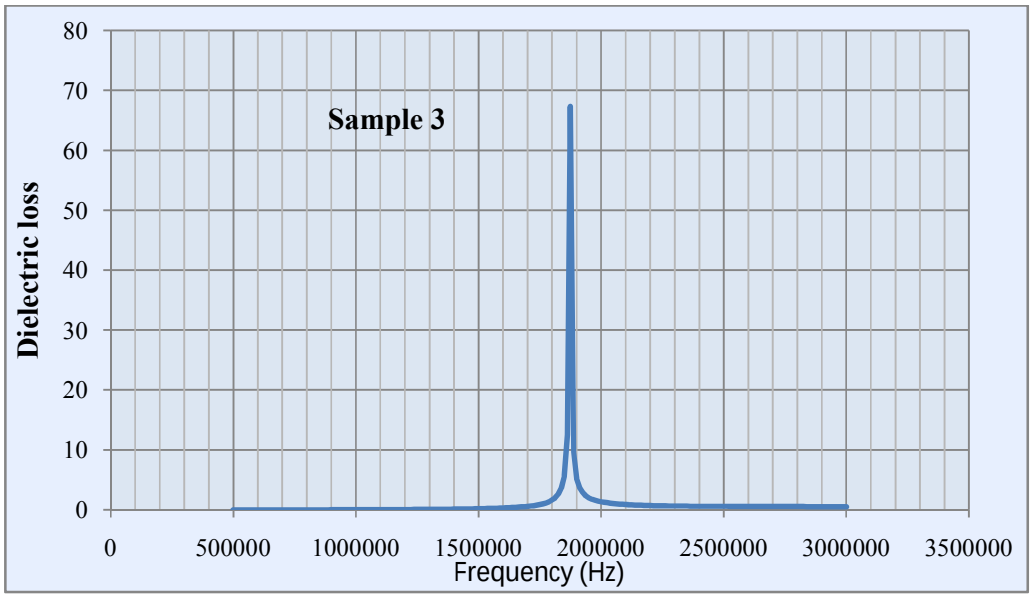

Figure 4.15 Variation of dielectric loss versus frequency for the sample no.3

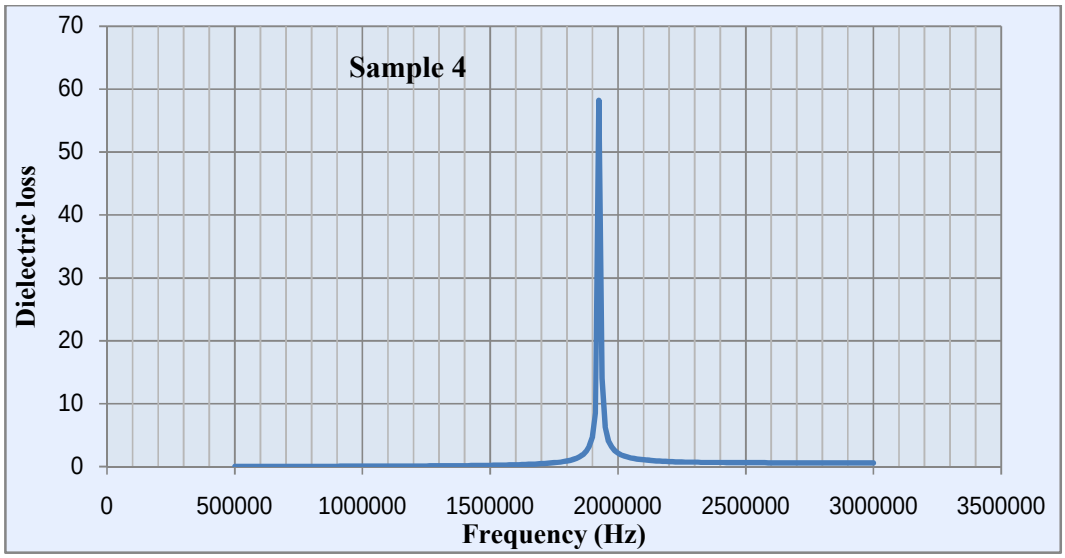

Figure 4.16 Variation of dielectric loss versus frequency for the sample no.4

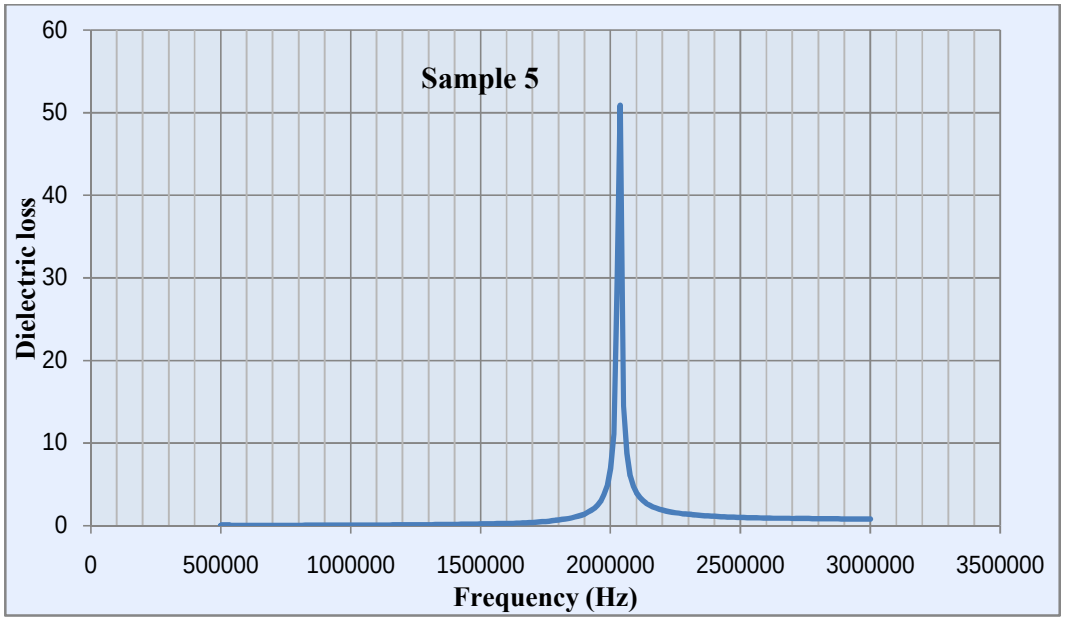

Figure 4.17 Variation of dielectric loss versus frequency for the sample no.5

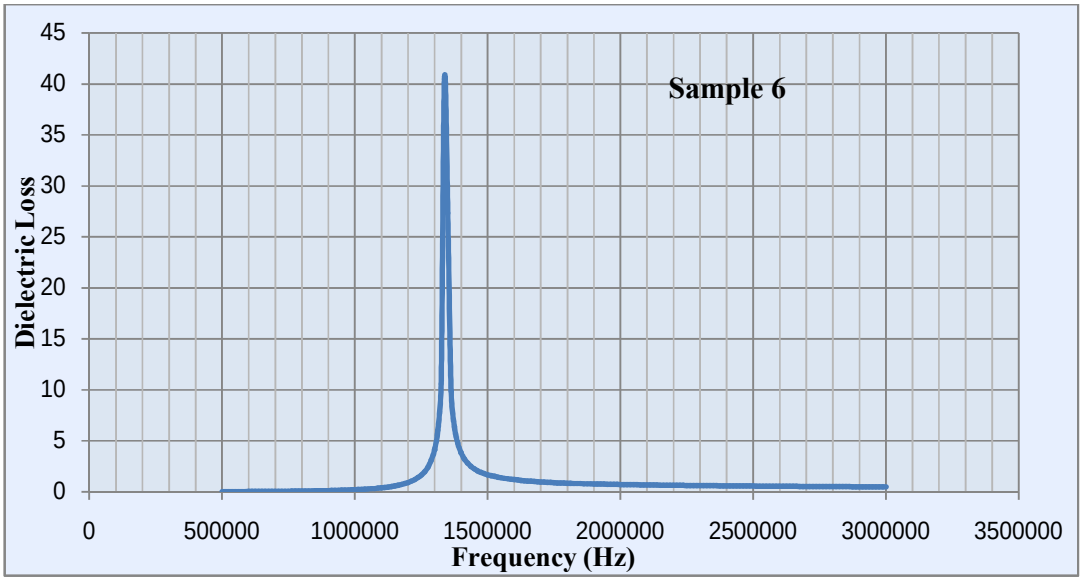

Figure 4.18 Variation of dielectric loss versus frequency for the sample no.6

The core loss of Mn-Zn ferrite is strongly dependent upon the capacitance of grain boundaries of sintered core. In frequency region between 0.5 MHz to 3 MHz the dielectric loss dominates the core loss. The power loss at the frequency higher than 1 MHz is influenced not only by the hysteresis and eddy current loss but also by dielectric loss. The dielectric loss is affected by grain boundary capacitance in the range from 0.5 MHz to 3MHz. In this study we reduced the dielectric loss by increasing the grain boundary impedance. At the middle high frequency region (1.8 MHz-2.3 MHz), the dielectric loss dominates the core loss. A slow variation of the dielectric loss tangent with the additives concentration has been found for all the samples. Additions of pentavalent ions such as Nb_2O_5 in Mn-Zn ferrites have been improve the core loss.

It is suggested that by decreasing the grain boundary capacitance at middle high frequency may improve the properties of the Mn-Zn ferrites and permits its applications in this frequency range.

CHAPTER 5

CONCLUSIONS

The present work reports the electrical and magnetic properties of a MnZn ferrite material of basic composition 52.5 mole% Fe_2O_3, 41.2 mole% MnO and 6.3 mole% ZnO with traces of some additives, suitable for power applications.

In order to improve the high frequency Mn-Zn power ferrite materials, it's necessary to add CaO and Nb_2O_5 according to the conditions of application to suppress the power losses. In this study, with the addition of CaO, the grain boundary resistivity of high frequency Mn-Zn power ferrite increased and the power loss declined. The suitable combination of this ferrite composition with 0.05% Calcium oxide, 0.02% Niobium oxide and 0.02% Zirconium oxide, processed under strictly controlled sintering profile results in the prospective material for power loss application. A power loss value of 137 kW/m^3 at 100 KHz, 80 ^oC and 100 mT, and of 309 kW/m^3 at 200 KHz, 100^oC and 100 mT respectively. The lowest power loss value is reported between 80-120 ^0C, Mn-Zn ferrite materials. Also the material is found to be suitable in the frequency of range of 0.5 MHz to 2.5 MHz and have the Curie temperature of approx.260^oC. The dielectric loss is affected by grain boundary capacitance in the range from 0.5 MHz to 3MHz. In this study we reduced the dielectric loss by increasing the grain boundary impedance.

Power loss of less than 350 kW/m^3 in the temperature range of 70-120 ^0C makes it the most promising candidate for being applicable in regular switching power supplies, as well as in main transformers in DC-DC converters for electrical vehicles such as hybrid electrical vehicles. This material can be shaped to any core design and can be used in the Inverter transformers for LCD backlight, AC adapters and chargers of notebook type PC's. The minimum power loss of the Mn-Zn ferrite is 260 kW/m^3 at 100 KHz, 120 ^oC. We concluded that this Mn-Zn ferrite worked at high temperature, some power devices such as lighting electronics and automotive electronics must work at higher temperature which is far above 100^oC.

CHAPTER 6

SCOPE OF THE FUTURE WORK

In response to the current demand for size reduction of electronic devices, the development of compact and efficient switched-mode-power supplies has received considerable attention. Power supplies being an integral part of electronic equipments from computers and microprocessors to TV and video tape-recorders, the demand for ferrite cores, which are an essential component of the switching power supplies, is continuously on the rise.

These modern devices exclusively need soft magnetic materials as its basic component. Soft ferrite material is extensively used in inductors, transformers, antenna rods, loading coils, deflection yokes, choke coils, recording heads, magnetic amplifiers, electromagnetic interference (EMI), power transformer and splitter applications, which forms a basic requirement in high technology areas. Mn–Zn ferrites adequately suit these demands and are considered to shape the future advanced technology.

Most soft ferrite for power application has a loss minimum between 80^{o}C and100^{o}C. And for safety reason their maximum working temperature is not above 100^{o}C. However, some power devices such as lighting electronics and automotive electronics must work at higher temperature which is far above 100^{o}C (some automotive electronics' working temperature reaches 150^{o}C). So ferrites used in these devices are requested to have good high temperature performance (for example high Bs and low core loss at high temperature). Mn-Zn ferrite material with these properties will certainly enhance fuel efficiency, electric-power saving, downsizing and weight saving.

References

1. Chikazumi, Physics of Magnetism, New York: John Wiley & sons (1964).
2. H. Tsunekawa, A. Nakata, T. Kamijo, K. Okutani, R. K. Mishara Mag. MAG-15(6).
3. A. Znidarsic, M. Limpel, M. Drofenik, "Effect of Dopants on the Magnetic Properties of MnZn Ferrites for High Frequency Power Supplies", IEEE Trans. Mag. 312, 950- 953 (1995)
4. M. Drofenik, A. Žnidaršič and I. Zajc, J. Appl. Phys. 82 (1997).
5. Satoshi Gotoh, Power and Magnetic materials lab Kawasaki steel.
6. Ke Sun, Zhongwen Lan, Zhong Yu, Lezhong Li, Xiaoliang Nie, Zhiyong Xu, Journal of Alloys and Compounds 468,315–320, (2009)
7. A. K. Singh, Abhishek K. Singh, T.C. Goelb, R.G. Mendiratta, Journal of Magnetism and Magnetic Materials 281, 276–280 (2004)
8. Y. Liu, S. He, Journal of Magnetism and Magnetic Materials 320 3318–3322 (2008)
9. R. Lebourgeois, J.P. Ganne and B.Lioret, Thomson-CSF/LCR, Domaine de Corbeville, 91404 Orsay cedex, France.
10. YU Zhong LAN Zhongwen WANG Jingmei ZHANG Yidong WANG Haocai (School of Microelectronics and Solid-State Electronics, UESTC Chengdu 610054 China).
11. A. Znidarsic, M. Limpel, G. Drazic, and M. Drofenik, in ''Ferrites: - Proceedings Of the Sixth International Conference on Ferrites, Tokyo,'' ICF6, p. 333, 1992.
12. K. Ishino, S. Satoh, Y. Takahashi, K. Iwasaki, and N. Obata, in ''Ferrites: Proceedings of the Sixth International Conference on Ferrites, Tokyo,'' ICF6. (1992).
13. S R Murthy Bull. Mater. Sci., Vol. 26, 99–503 (2003)
14. Weon Hee JEONG and Young Ho HAN, Department of materials engineering, Sungkyunkwan University, 300 Chunchun-dong, jangan-gu, Suwon, Korea.
15. S. Bharadwaj, K. Praveena, K. Sadhana, S.R. Murthy Department of Physics, Osmania University, Hyderabad 500007, India.
16. Y.H. Han, J.J. Suh, M.S. Shin and S.K. Han, Sung Kyun Kwan University, 300 Chunchun-Dong, Suwon, Korea.

17. A. Verma, M.I. Alam, R. Chatterjee, T.C. Goel, R.G. Mendiratt Journal of Magnetism and Magnetic Materials 300, 500–505, 2006

18. A. Znidarsic, M. Limpel, G. Drazic, and M. Drofenik, in ‘‘Ferrites: - Proceedings of the Sixth International Conference on Ferrites, Tokyo,’’ ICF6, p. 333, 1992.
19. V.T. Zaspalis, The effect of Nb2O5 dopants on the structural and magnetic Properties of MnZn-ferrites, Journal of Magnetism and Magnetic Materials 250 (2002) 98–109.
20. J. T’opfer, Microstructural effects in low loss power ferrites, Journal of the European Ceramic Society 25 (2005) 3045–3049.
21. B. P. Rao, K. H. Rao, G. Sankaranarayana, A. Padurarua, O. F. Caltuna Department of Physics, Andhra University, Visakhapatnam 530003, India